REFORM-EVAL: EVALUATING LARGE VISION LANGUAGE MODELS VIA UNIFIED RE-FORMULATION OF TASK-ORIENTED BENCHMARKS

Zejun Li[1†], Ye Wang[1†], Mengfei Du[1†], Qingwen Liu[1†], Binhao Wu[1†], Jiwen Zhang[1†], Chengxing Zhou[2], Zhihao Fan[3], Jie Fu[4], Jingjing Chen[1], Xuanjing Huang[1], Zhongyu Wei[1*]
[1]Fudan University [2]Northeastern University [3]Alibaba Group
[4]Hong Kong University of Science and Technology
zejunli20@fudan.edu.cn zywei@fudan.edu.cn
https://github.com/FudanDISC/ReForm-Eval

ABSTRACT

Recent years have witnessed remarkable progress in the development of large vision-language models (LVLMs). Benefiting from the strong language backbones and efficient cross-modal alignment strategies, LVLMs exhibit surprising capabilities to perceive visual signals and perform visually grounded reasoning. However, the capabilities of LVLMs have not been comprehensively and quantitatively evaluated. Most existing multi-modal benchmarks require task-oriented input-output formats, posing great challenges to automatically assess the free-form text output of LVLMs. To effectively leverage the annotations available in existing benchmarks and reduce the manual effort required for constructing new benchmarks, we propose to re-formulate existing benchmarks into unified LVLM-compatible formats. Through systematic data collection and reformulation, we present the ReForm-Eval benchmark, offering substantial data for evaluating various capabilities of LVLMs. Based on ReForm-Eval, we conduct extensive experiments, thoroughly analyze the strengths and weaknesses of existing LVLMs, and identify the underlying factors. Our benchmark and evaluation framework will be open-sourced as a cornerstone for advancing the development of LVLMs.

1 INTRODUCTION

With the trend led by ChatGPT (OpenAI, 2023a), LLMs (Large Language Models) (OpenAI, 2023b; Touvron et al., 2023a; Chiang et al., 2023) have ushered in revolutionary advancements in Natural Language Processing (NLP). Inspired by these efforts, researchers attempt to extend the success of LLMs to the realm of vision language. By equipping LLM with visual encoders and aligning multi-modal representations through generative pre-training, large vision language models (LVLMs) (Li et al., 2023b; Liu et al., 2023b; Zhu et al., 2023; Ye et al., 2023) possess the capability to comprehend visual information and engage in multi-modal conversations with users.

However, the reliability of such LVLMs remains a mystery. On the one hand, these models demonstrate surprising abilities like OCR (Liu et al., 2023d), meme understanding (Zhu et al., 2023), and visual commonsense reasoning (Li et al., 2023b). On the other hand, LVLMs suffer from fundamental issues, such as object hallucination (Li et al., 2023d). Meanwhile, due to the lack of suitable benchmarks, there is a shortage of quantitative analysis and comparison of LVLMs.

The main reason for this situation is the structural gap between existing task-oriented multi-modal benchmarks and LVLMs. Most existing benchmarks are designed for specific tasks and demand highly structured input-output formats (Lin et al., 2014). For instance, VQA v2 (Goyal et al., 2017) requires concise answers, typically in the form of single words or short phrases. Previously evaluated vision-language pre-trained models (Chen et al., 2020; Zhang et al., 2021) need to be fine-tuned and

*Corresponding author.
†These authors contributed equally to this work.

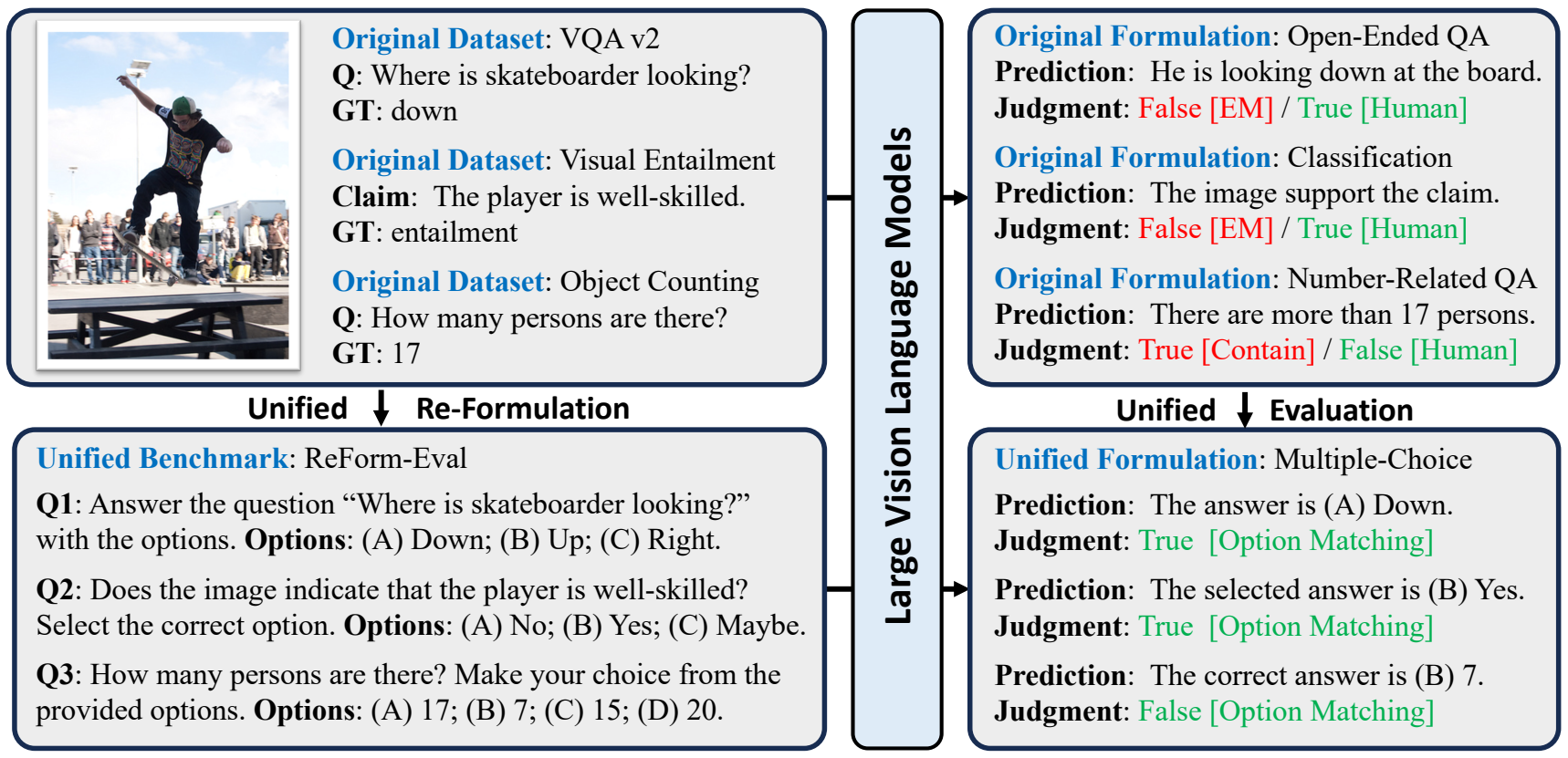

Figure 1: Illustration of the unified re-formulation of existing benchmarks into multiple-choice problems. The text within square brackets indicates the evaluation methods, with red and green denoting incorrect and correct judgment, respectively. "EM" is short for exact match.

learn task-specific parameters to fit the structures of such benchmarks. On the contrary, LVLMs are flexible and tend to provide detailed responses, even for yes-or-no questions. As depicted in the flowchart in the upper part of Figure 1, such gap poses the greatest obstacle to accurate automated evaluation, particularly when assessing the desired zero-shot capabilities.

To bridge the structure gap, we explore ways of re-formulating existing benchmarks into unified formats that are compatible with LVLMs. Referring to Figure 1, we adapt the evaluation process to the unified form shown in the lower part. Multi-modal benchmark datasets are re-formulated as multiple-choice problems or specialized text generation problems. Datasets for tasks with specific text generation requirements, like OCR and image captioning, are re-formulated as specialized text generation problems. Other datasets are restructured into multiple-choice problems.

The unified formulation enables universal and comprehensive evaluation. For each formulation, we design a consistent and reliable evaluation method. As mentioned in (Fu et al., 2023), current LVLMs may struggle to follow multiple-choice instructions, we propose both black-box and white-box approaches to assist: (1) Guiding LVLMs to output in desired formats through in-context-learning; (2) Directly calculating the generation probability for options and selecting the one with the highest value. Considering the sensitivity of LVLMs to the input prompts (Zeng et al., 2023), we design an instability-aware evaluation strategy and introduce a metric to characterize such instability.

Based on the re-formulation framework, we present our unified multi-modal benchmark, ReForm-Eval. For a comprehensive evaluation, we re-formulate 61 benchmark datasets based on existing data resources, the evaluation dimensions range from basic visual perception to high-level visual reasoning and dialog. Compared with recent LVLM benchmarks that require manual annotation (Fu et al., 2023; Liu et al., 2023c), ReForm-Eval fully utilizes publicly open resources and provides significantly more data, almost 100 times the size of MMBench. Meanwhile, unlike LVLM-ehub (Xu et al., 2023), which requires designing complex and dataset-specific evaluation strategies, ReForm-Eval offers greater scalability and a more universally applicable and efficient evaluation approach.

Based on ReForm-Eval, we conduct a comprehensive evaluation of 16 open-source LVLMs across various capability dimensions. We hope ReForm-Eval and the associated findings can constitute a valuable augmentation to the ongoing efforts in LVLM research and development.

2 Related Works

2.1 Large Vision Language Models

Inspired by the advancements of LLMs and the multi-modal understanding abilities demonstrated by GPT-4 (OpenAI, 2023b), developing open-source LVLMs currently dominates the multi-modal research. Visual signals encoded by visual encoders (Radford et al., 2021) are incorporated in LLMs through linear projection (Tsimpoukelli et al., 2021), Q-former (Li et al., 2023b), or cross-attention layers (Alayrac et al., 2022). To enable multi-modal instruct tuning, MiniGPT4 (Zhu et al., 2023) bootstraps high-quality data by refining the previous output, LLaVA (Liu et al., 2023b) proposes to

employ GPT-4 to generate image-involved dialogs while other works construct instruct tuning data from existing vision-language benchmarks (Xu et al., 2022; Dai et al., 2023; Li et al., 2023c).

To seamlessly adapt LLMs for multi-modal scenarios, many efforts are paid including designing strategies for parameter freezing (Ye et al., 2023), introducing light-weight trainable modules into the backbone (Gong et al., 2023; Gao et al., 2023), incorporating continuous output (Peng et al., 2023; Chen et al., 2023), and enhancing the visual representations (Zeng et al., 2023; Hu et al., 2023; Li et al., 2023a). Benefiting from the aligned representations from ImageBind (Girdhar et al., 2023), LVLMs can be further extended to more modalities (Han et al., 2023; Su et al., 2023).

However, the capabilities of existing LVLMs are mainly demonstrated by qualitative examples (Zhu et al., 2023; Su et al., 2023; Gong et al., 2023). To our knowledge, few benchmarks are suitable for evaluating the capabilities of LVLMs, hindering quantitative analysis and comparison of LVLMs.

2.2 Multi-Modal Benchmarks

Task-Oriented Benchmarks Most existing multi-modal benchmarks can not be directly utilized to evaluate LVLMs since they are designed for specific tasks and rely on structured input-output formats for evaluation. VQA v2 (Goyal et al., 2017) requires concise answers, retrieval benchmarks (Lin et al., 2014; Young et al., 2014) demand dense scores for all image-text pairs, VCR (Zellers et al., 2019) provides coordinates to refer visual object in the question, and bounding box output is necessary for RefCOCO (Kazemzadeh et al., 2014). This characteristic makes it challenging to utilize such benchmarks to evaluate the free-form text outputs of LVLMs unless complex post-processing and evaluation methods are designed specifically (Xu et al., 2023; Yin et al., 2023).

Benchmarks for LVLMs To facilitate reliable and efficient automated evaluation of LVLMs, efforts are paid to construct LVLM-compatible benchmarks, such as yes-or-no problems in MME (Fu et al., 2023) and multiple-choice problems in MMBench (Liu et al., 2023c). A portion of the benchmarks are designed to assess specific capabilities (Liu et al., 2023d; Wang et al., 2023) or diagnose particular issues (Li et al., 2023d; Zhao et al., 2023), while others aim for comprehensive evaluation (Fu et al., 2023; Liu et al., 2023c). However, limited manual annotation (around 100 samples per dimension in MME and MMBench) could potentially introduce evaluation bias into the results.

3 ReForm-Eval Benchmark

In this section, we describe how to construct ReForm-Eval by re-formulating existing task-oriented multi-modal benchmarks. Section 3.1 introduces the general framework of re-formulation. Section 3.2 summarizes the capability dimensions assessed in ReForm-Eval and corresponding datasets. Section 3.3 illustrates the methods and strategies used to evaluate LVLMs based on ReForm-Eval.

3.1 Unified Re-Formulation Framework

Existing LVLMs primarily adopt LLMs as backbones and use free-form text to interact with users. This paradigm makes the output more flexible and aligned with human needs. However, the gap between these models and existing highly structured benchmarks poses challenges for evaluation. In order to effectively reuse the annotations in existing benchmarks, these benchmarks need to be re-formulated into appropriate formats. Motivated by benchmarks for LLMs (Hendrycks et al., 2020; Srivastava et al., 2022; Huang et al., 2023), ReForm-Eval considers two formats that are compatible with LVLMs, namely multiple-choice problems and text-generation problems.

Multiple-choice problem is the primary format in ReForm-Eval. By providing options for the questions, models are guided to produce responses in a constrained format. The key in multiple-choice problem construction is how to prepare meaningful negative options. Generally, for close-vocabulary classification tasks, we build relationships between categories based on which hard negative options are selected. For open-ended tasks, based on the question and the correct answer, negative options can be obtained with the help of task-specific strategies or LLMs like ChatGPT.

For OCR and image captioning that involves text generation, corresponding benchmarks are formulated as text-generation problems tailored to various scenarios. We curate the input prompts to

describe the tasks and requirements. For OCR tasks, responses should contain the target tokens in the image. For description tasks, models should provide concise depictions of the visual content.

3.2 Evaluation Dimensions

To address the wide range of questions posed by users, LVLMs need to possess diverse capabilities. For a comprehensive evaluation, we curate 61 benchmark datasets from existing resources, summarizing the assessed capabilities into 2 major categories and 8 sub-categories which are illustrated in Figure 2. To avoid information overload, details about the re-formulation procedures and dataset statistics are provided in Appendix A.

3.2.1 Visual Perception Tasks

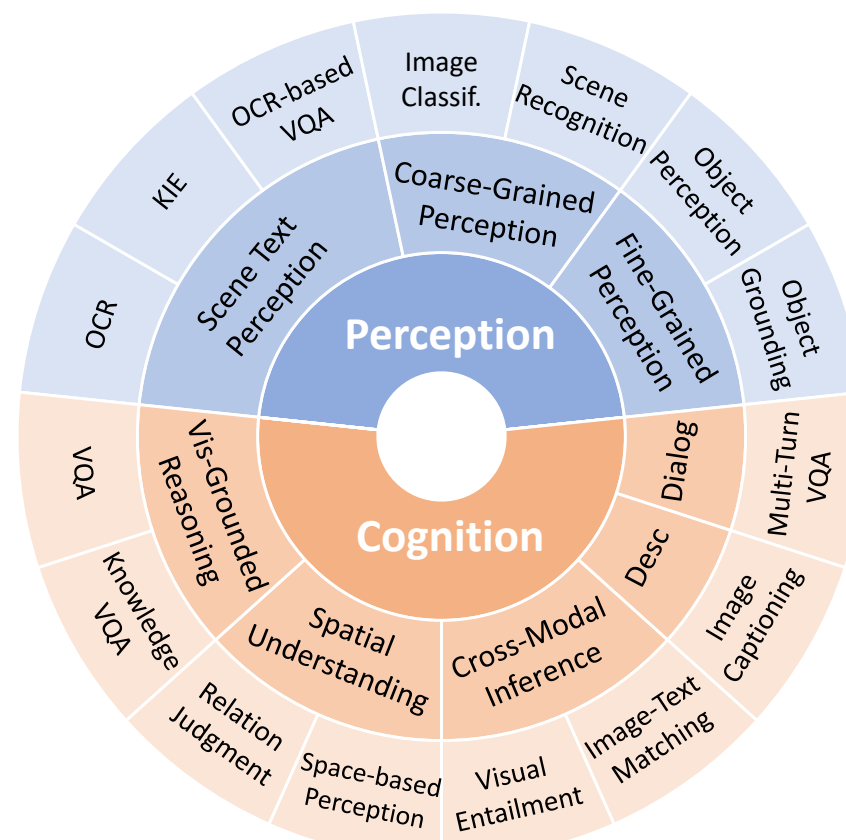

Figure 2: Assessed capability dimensions and tasks in ReForm-Eval. "Desc" and "Classif" are respectively short for description and classification.

Coarse-Grained Perception (CG) Coarse-grained perception is the ability to recognize the overall layout and main objects at the image level. We evaluate this capability through ***image classification*** using Flowers102 (Nilsback & Zisserman, 2008), CIFAR10 (Krizhevsky et al., 2009), ImageNet-1K (Deng et al., 2009), Pets37 (Parkhi et al., 2012), and MEDIC (Alam et al., 2023) benchmarks, and ***scene recognition*** using TDIUC (Kafle & Kanan, 2017) and VizWiz (Gurari et al., 2018) benchmarks. The samples are re-formulated as multiple-choice questions.

Fine-Grained Perception (FG) Fine-grained perception requires detailed sensing at the object level. We set up the ***object perception*** task (using TDIUC (Kafle & Kanan, 2017) and MSCOCO (Lin et al., 2014) benchmarks) and the ***object grounding*** task (using MSCOCO (Lin et al., 2014) and RefCOCO (Yu et al., 2016) benchmarks) for evaluation. Object perception measures how well a LVLM can identify local semantics, while object grounding assesses the ability to localize fine-grained objects. All tasks are formulated as multiple-choice questions.

Scene Text Perception (STP) Scene text perception enables LVLMs to identify, understand, and perform inference based on text in images. This evaluation is conducted through ***optical character recognition*** (OCR) using 6 benchmarks (including CUTE80 (Risnumawan et al., 2014), IC15 (Karatzas et al., 2015), IIIT5K (Mishra et al., 2012), COCO-Text (Mishra et al., 2012), WordArt (Xie et al., 2022), TextOCR (Singh et al., 2021)), ***key information extraction*** (KIE) using 3 benchmarks (including SROIE (Huang et al., 2019), POIE (Kuang et al., 2023) and FUNSD (Jaume et al., 2019)) and ***OCR-based VQA*** using 3 benchmarks (including TextVQA (Singh et al., 2019), DocVQA (Mathew et al., 2021) and OCR-VQA (Mishra et al., 2019)). We consider STP as a specialized text-generation problem that requires output to contain exactly matched words.

3.2.2 Visual Cognition Tasks

Visually Grounded Reasoning (VGR) A reliable LVLM is supposed to perform reasoning based on multi-modal contextual information. In order to assess such capability, we adopt the commonly applied ***visual question answering*** (VQA) task and its variant, ***knowledge-based visual question answer*** (K-VQA), which further requires models to utilize internally stored knowledge. For vanilla VQA, we adopt VQA v2 (Goyal et al., 2017), GQA (Hudson & Manning, 2019), and Whoops (Bitton-Guetta et al., 2023). As for KVQA, we consider 6 benchamrks including OK-VQA (Marino et al., 2019), ScienceQA (Lu et al., 2022), VizWiz (Gurari et al., 2018), ViQuAE (Lerner et al., 2022), A-OKVQA (Schwenk et al., 2022) and ImageNetVC (Xia et al., 2023). The aforementioned benchmarks are re-formulated into multiple-choice questions.

Spatial Understanding (Spatial) Spatial understanding is the key to the real-life application of LVLMs on robots. This task requires a comprehensive understanding of both the object-object and

object-observer relationship so as to make reasonable behaviors. We access such capability through ***spatial relation judgment*** (SRJ) using VSR (Liu et al., 2023a) and MP3D-Spatial, a benchmark designed for embodied tasks in real-world environments, constructed from Matterport3D (Chang et al., 2017). Additionally, we employ ***Space-Based Reasoning*** (SBR) through the CLEVR (Johnson et al., 2017) benchmark. The SRJ task aims to accurately identify spatial relationships, forming a concept of where the ego is in space. The SBP task entails complex reasoning ability based on the understanding of spatial relationships. All samples are re-formulated as multiple-choice questions.

Cross-Modal Inference (CMI) A thorough comprehension of both modalities is required to perform cross-modal inference on the relationship between images and texts. We consider two tasks: ***image-text matching*** (ITM) requires models to measure the cross-modal similarities and ***visual entailment*** (VE) demands models to check whether the information is entailed across modalities. MSCOCO (Lin et al., 2014), WikiHow (Koupaee & Wang, 2018), Winoground (Thrush et al., 2022) are adopted for ITM while VE considers SNLI-VE (Xie et al., 2019) and MOCHEG (Yao et al., 2023). Both tasks are re-formulated as multiple-choice questions.

Visual Description (Desc) Visual description is an inherent capability of LVLMs as generative models. We adopt the ***image captioning*** task on MSCOCO (Lin et al., 2014), TextCaps (Sidorov et al., 2020), NoCaps (Agrawal et al., 2019), and Flickr30K (Young et al., 2014) for evaluation. These datasets are formulated as text-generation problems with the requirement of concise outputs.

Multi-Turn Dialogue (Dialog) Existing benchmarks primarily focus on single-turn conversation. ReForm-Eval evaluates the performance of LVLMs in multi-turn dialogues. We consider the ***multi-turn VQA*** task using VisDial (Das et al., 2017) and VQA-MT, the latter is constructed by reorganizing questions in VQA v2. Both benchamrks are formulated as multiple-choice questions.

3.3 Evaluation Strategy

3.3.1 Evaluation Methods and Metrics

With the unified problem formulation, the performance of LVLMs can be universally evaluated. For specialized text-generation problems, the evaluation method depends on the scenario. For visual description, we follow Li et al. (2023b) to use CIDEr (Vedantam et al., 2015) as the evaluation metric. Since the adopted datasets mainly provide concise references, we craft the prompt to require concise responses and restrict the maximum number of tokens a model can generate. As for STP, input prompts are well-designed to instruct models to identify the scene texts. The evaluation metric is word-level accuracy: the proportion of ground-truth words that appear complete in the output.

Considering multiple-choice problems, the model performance is assessed using accuracy. We label the answer options with markers like "(A)" and then determine correctness by checking the markers in the output of models. The challenge with this approach is that current LVLMs may not always adhere well to multiple-choice instructions, i.e. the output may not include the required marker.

To assist in the evaluation of multiple-choice problems, ReForm-Eval provides both a black-box method and a white-box method. The black-box method provides in-context samples to guide LVLMs to generate responses in desired formats. Here is an example of the input prompt:

$X_{\text{system-message}}$
Human: Can you see the image? Options: (A) Yes; (B) No; (C) Not Sure; (D) Maybe.
Assistant: The answer is (A) Yes.
Human: X_{question} Options: X_{options}
Assistant: The answer is

where $X_{\text{SystemMessage}}$ is the system message required by most LVLMs, X_{question} and X_{options} are respectively the question and the answer options described in text, the text in red is the in-context sample provided to the model. Notice that the in-context sample provides no information about the image. The effectiveness of the black-box strategy is demonstrated in Section 4.3.3.

The white-box approach is based on the inherent attribute of current LVLMs as generative models. Given the visual context v, the question q, and N answer options $C = \{c^i\}_{i=1}^N$, the answer prediction

Model	Generation Evaluation									Likelihood Evaluation						
	Perception			Cognition					$\bar{R}$	Perception		Cognition				$\bar{R}$
	CG	FG	STP	Spatial	VGR	Dialog	CMI	Desc		CG	FG	Spatial	VGR	Dialog	CMI	
BLIP-2$_F$	69.4	76.6	38.1	43.2	73.3	**61.8**	66.9	**74.3**	2	60.7	74.4	51.1	69.8	62.6	58.9	4
InstructBLIP$_F$	**71.2**	**78.1**	**41.2**	**46.1**	**73.9**	60.6	**71.4**	43.8	**2**	60.4	75.6	51.2	71.0	67.2	55.5	4
InstructBLIP$_V$	69.1	70.8	40.7	44.4	63.0	48.6	53.8	27.3	4	58.5	77.8	52.3	**73.5**	**68.7**	55.4	3
LLaVA$_V$	28.7	34.4	18.4	28.7	44.0	35.6	47.3	36.8	11	61.0	70.3	42.4	58.9	52.3	48.0	8
LLaVA$_{L_2}$	48.3	59.8	21.5	41.2	59.7	46.3	49.9	39.5	6	49.9	65.6	47.4	56.7	48.6	49.7	11
MiniGPT4	46.2	53.2	33.0	34.6	45.6	39.5	45.4	47.5	7	54.9	70.6	49.2	57.3	54.1	50.9	8
mPLUG-Owl	42.0	37.2	39.8	26.8	37.5	35.2	40.4	44.7	11	57.9	66.1	48.6	54.3	45.5	49.8	10
PandaGPT	28.2	34.6	4.5	33.3	41.9	34.1	36.6	1.6	14	42.3	47.4	39.4	43.3	41.5	37.0	16
IB-LLM	29.2	32.7	8.2	35.6	36.7	35.3	36.6	27.6	13	49.6	54.4	46.1	50.3	39.5	45.6	15
LA-V2	33.2	30.8	24.2	23.8	36.3	35.4	41.1	36.0	13	42.7	61.4	48.6	54.1	43.4	49.9	12
mmGPT	30.4	30.3	16.7	26.9	33.0	31.8	38.2	27.7	14	52.6	62.4	47.2	56.2	43.1	44.1	13
Shikra	47.2	47.5	8.3	33.3	41.2	35.2	44.5	31.8	11	60.9	66.8	45.5	58.5	59.5	**59.3**	7
Lynx	59.5	62.6	18.6	40.2	58.4	47.0	53.0	60.7	5	**66.1**	76.2	**53.9**	69.9	60.0	57.4	3
Cheetor$_V$	52.0	50.3	25.9	30.6	49.9	40.3	47.4	61.6	7	56.1	69.0	48.4	58.7	57.6	50.6	8
Cheetor$_{L_2}$	46.5	51.4	18.8	34.5	54.4	40.6	44.0	43.9	8	61.6	56.1	48.7	57.5	46.8	47.2	11
BLIVA	41.7	43.4	40.8	33.3	42.4	39.8	45.2	52.5	8	64.9	**78.2**	51.7	72.9	68.1	53.7	**2**

Table 1: General evaluation results of LVLMs across different capability dimensions. "CG", "FG", "CMI", and "Desc" are respectively short for coarse-grained perception, fine-grained perception, cross-modal inference, and description. "$\bar{R}$" represents the average rank across dimensions.

can be determined by the generation likelihood predicted by the evaluated model:

$$\hat{c} = \arg\max_{c^i \in C} P_\theta(c^i|v,q) = \arg\max_{c^i \in C} \sum_{t=1}^{t_c} P_\theta(c^i_t|v,q,c^i_{<t}) \quad (1)$$

where $P_\theta(c^i_t|v,q,c^i_{<t})$ is parameterized by the causal-LLM-based LVLMs and $\{c^i_1,...,c^i_{t_c}\}$ is the tokenized sequence of c^i. For multiple-choice problem assessment, we provide both the black-box generation evaluation results and the white-box likelihood evaluation results.

3.3.2 Instability-Aware Evaluation

As demonstrated in previous work (Xu et al., 2022; Zeng et al., 2023), LLM-based models are sensitive to the different but equivalent instructions. In ReForm-Eval, instability-aware evaluation is thus introduced. For each task, multiple (more than five) instruction templates are manually designed. Each sample is tested multiple times with different templates and shuffled options if it is a multiple-choice question. The final result is based on the average of the multiple tests.

To directly characterize the instability of models, we further introduce a metric. For a multiple-choice problem with answer options $C = \{c^i\}_{i=1}^N$, the empirical prediction distribution of a model can be calculated from the M tests as $p_i = \frac{1}{M}\sum_{j=1}^M \mathbb{1}(\hat{c}_j = c^i)$ where $\hat{c}_j$ is the prediction of the j-th test. Then the instability is measured by the entropy of the prediction distribution: $e = -\sum_{i=1}^N p_i \log(p_i)$. Larger e indicates higher uncertainty in the predictions for that sample. For text-generation tasks, instability is not accessible as the prediction distribution is not directly measurable.

4 Experiments

4.1 Implementation Details

Based on ReForm-Eval, we evaluate 16 models with around 7B parameters that are trained with 13 different methods, including BLIP-2 (Li et al., 2023b), InstructBLIP (Dai et al., 2023), LLaVA (Liu et al., 2023b), MiniGPT4 (Zhu et al., 2023), mPLUG-Owl (Ye et al., 2023), PandaGPT (Su et al., 2023), ImageBind-LLM (IB-LLM) (Han et al., 2023), LLaMA-Adapter V2 (LA-V2) (Gao et al., 2023), multimodal-GPT (mmGPT) (Gong et al., 2023), Shikra (Chen et al., 2023), Lynx (Zeng et al., 2023), Cheetor (Li et al., 2023a), BLIVA (Hu et al., 2023). Details of the methods are introduced in Appendix B.2. All experiments are conducted in the same software and hardware environment to ensure fairness. For specific parameter settings, please refer to Appendix B.1.

Notations For models with multiple variants based on different backbones, we use subscripts to denote the backbone used: F, V, L, and L_2 represent FlanT5, Vicuna, LLaMA, and LLaMA2, respectively. For multiple-choice problems, "Generation Evaluation" and "Likelihood Evaluation"

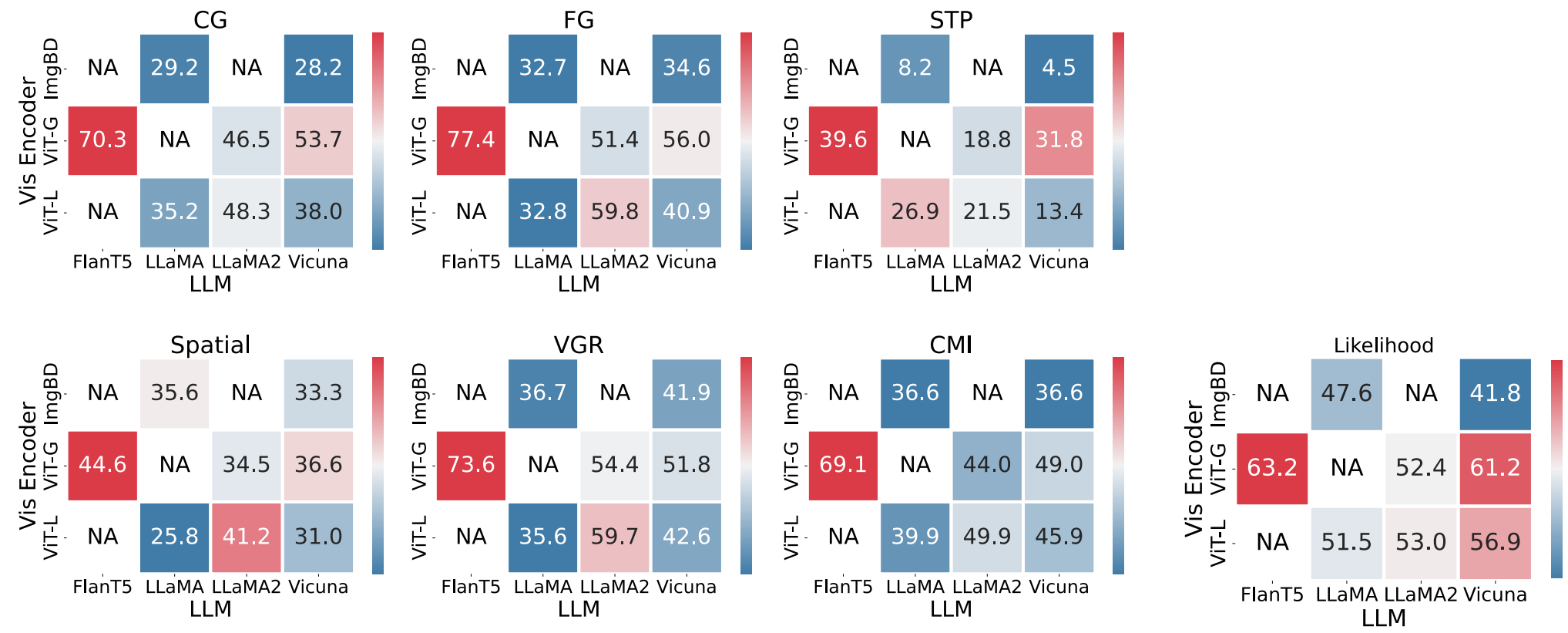

(a) Generation (b) Likelihood

Figure 3: The influence of different language and visual backbones. For generation evaluation, we average the results of various models based on the backbone used. To better visualize the results, we selected heatmaps across six dimensions (dialog and desc are omitted). For likelihood evaluation, we further compute the average score across dimensions since the performance trend is consistent. Note that "ImgBD" is short for ImageBind in this figure.

Visual Backbone		**ImageBind**		**ViT-G**		**ViT-L**		
Connection Arch		BindNet+Gate	Linear	Perceiver	Q-Former	Adapter	Linear	Perceiver
Generation	Perception	23.4	22.4	46.9	50.4	29.4	34.9	32.7
	Cognition	34.3	29.5	51.9	49.3	34.5	41.0	34.2
Likelihood	Perception	31.0	31.4	61.1	58.6	32.0	44.3	35.0
	Cognition	36.0	36.5	49.7	49.1	34.2	42.3	33.7

Table 2: Average evaluation performance categorized by connection modules (see Table 7 for more details) and visual backbones under generation and likelihood strategy.

are respectively based on the black-box and white-box strategies. For each task under different strategies, the best result is marked in **bold** while the runner-up is underlined.

4.2 General Performance

Table 1 presents the comprehensive performance of each model across dimensions, from which several insights can be gleaned. (1) BLIP-2 and InstructBLIP continue to hold the top-2 positions in most dimensions, but in some individual dimensions, Lynx, BLIVA, and Shikra also take the lead. (2) It's worth noting that the effectiveness of models like BLIVA and Lynx only becomes apparent when using likelihood evaluation. We suspect this is attributed to the instruction-following ability of models, please refer to Section 4.3.4 for a detailed analysis. (3) Compared to models based on CLIP visual encoders, PandaGPT and IB-LLM, which are based on the ImageBind encoder, exhibit relatively poorer performance in image-text tasks. Meanwhile, most top-performing models utilize Vicuna and FlanT5 as the backbone. Further analysis is available in Section 4.3.1 regarding the impact of model architecture and backbones. (4) Apart from the architecture, a common characteristic among BLIP-2, InstructBLIP, Lynx, and BLIVA is the use of relatively high-quality data during pre-training. For data-related analysis, please refer to Section 4.3.2.

4.3 Comprehensive Analysis

4.3.1 Explore the Model Architecture

Model Backbone To gain a better insight into the backbone influence, we group models based on the backbone, as illustrated in Figure 3. For language backbones, Vicuna-based models outperform LLaMA-based models, whereas LLaMA2 and Vicuna excel in different dimensions. Under likelihood evaluation, Vicuna consistently performs better. FlanT5 seems the best, as the related models are BLIP-2 and InstructBLIP. Regarding visual backbones, ViT-G (from EVA-CLIP (Sun et al., 2023)) generally outperforms ViT-L (from CLIP (Radford et al., 2021)), which in turn outperforms ImageBind. Furthermore, LLaMA2 tends to favor smaller visual encoders like ViT-L, while Vicuna performs better when paired with larger visual encoders like ViT-G.

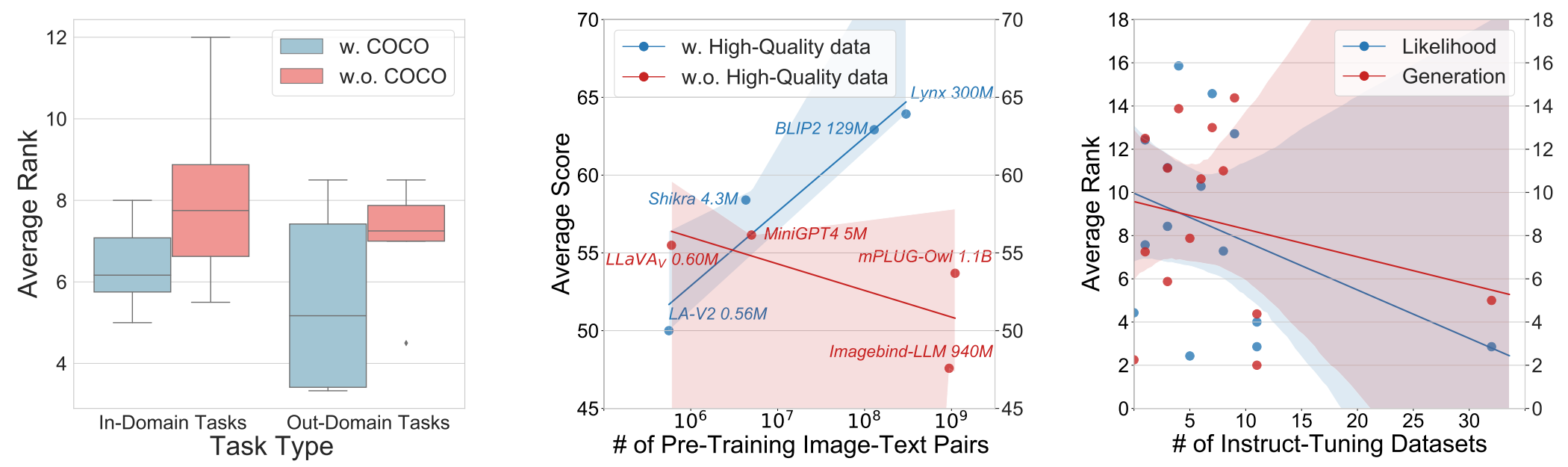

(a) (b) (c)

Figure 4: The influence of datasets in the pre-training and instruct-tuning stages. (a) compares the average rank of models pre-trained with and without the MSCOCO dataset. (b) shows the relationship between the scale of pre-training data and the average performance score of models grouped by data quality. (c) shows the relations between the number of instruct-tuning datasets and the average rank. The shaded area represents the 95% confidence interval.

Connection Module We further analyze the effect of connection modules in Table 2. ImageBind appears to perform subpar regardless of the choice of connection module. For larger visual backbones like ViT-G, both Perceiver and Q-Former show decent performance. For smaller visual backbones (ViT-L), Linear connection module is consistently better.

In summary, **language backbones are supposed to possess strong instruction-following capabilities. As for visual backbones, it's advisable to choose ViT-G and carefully select a connection module compatible with the corresponding visual backbone.** Besides, different model architectures result in varying parameter quantities. We discuss the impact in Appendix C.3.

4.3.2 Explore the Dataset

High-Quality Pre-training Dataset MSCOCO (Lin et al., 2014) is a typical high-quality human-annotated dataset that is commonly used during pre-training. To quantitatively assess its impact, we compare the average performance between models pre-trained with and without MSOCO. As shown in Figure 4 (a), MSCOCO not only helps with in-domain tasks but also enhances generalization results on out-domain tasks. Therefore, to effectively align cross-modal representations during pre-training, it is crucial to include such high-quality pre-training data.

Scaling Up Pre-Training Dataset To scale up the LVLM training, it is necessary to utilize image-text pairs crawled from the web. Figure 4 (b) compares two groups of models: the red-marked group uses data filtered based on rules or CLIP, such as CC (Sharma et al., 2018) and LAION (Schuhmann et al., 2021), while the blue-mark utilizes relatively high-quality data including aforementioned annotated data and synthetic captions from BLIP (Li et al., 2022). Results show that it is more effective to scale up utilizing synthetic data, resulting in a desired increasing curve. We believe the reason behind this is that synthetic captions are cleaner and more associated with images. While the diversity of data may be impaired, the generalizable backbones mitigate the negative impact.

Instruct-Tuning Dataset We also explore the impact of the number of instruct-tuning datasets. The fitted curve in Figure 4 (c) demonstrates that increasing the number of instruct-tuning datasets leads to improved performance of LVLMs. However, most existing LVLMs have only been trained on a small number of datasets and tasks, which limits their performance.

In general, **the quality of pre-training data and the diversity of instruct-tuning data are crucial factors for improving LVLMs**. Appendix C.4 provides the complete data used in this section.

4.3.3 Effect of In-Context Sample

To demonstrate the effectiveness of the black-box evaluation strategy introduced in Section 3.3.1. We assess LVLMs' ability to follow multiple-choice instructions under different strategies. The

Backbone	LLaMA-7B		Vicuna-7B		Vicuna-7B+		FlanT5-xl		Vicuna-7B+LoRA
Model	LA-V2	mPLUG-Owl	MiniGPT4	Cheetor	Shikra	LLaVA	BLIP-2	InstructBLIP	PandaGPT
Hit Rate	85.14	62.86	100	99.97	65.42	85.32	100	99.99	99.41
Hit Rate+	100	100	100	100	100	100	100	100	99.97

Table 3: Instruction-following ability of LVLMs in multiple-choice problems. "Vicuna-7B+" indicates the LLM backbone is fine-tuned. "Hit Rate" and "Hit Rate+" represent the format hit rate without and with in-context samples, respectively.

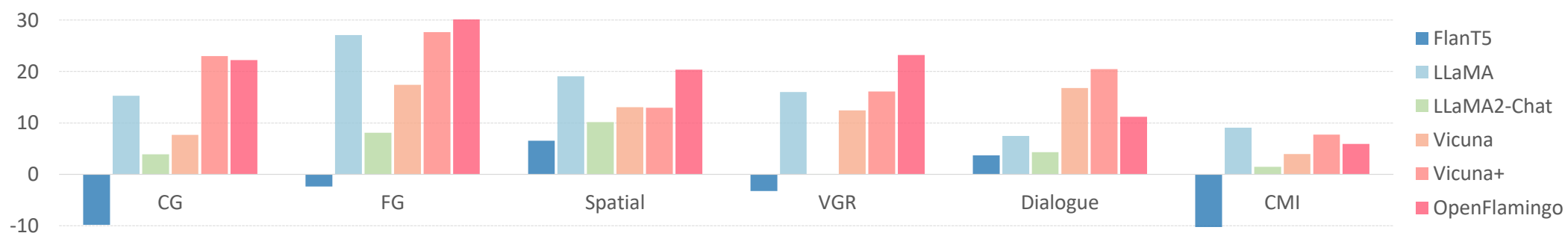

Figure 5: Performance gap of models under different evaluation strategies, grouped and averaged based on the language backbone. The vertical axis indicates how much the likelihood evaluation surpasses the generation evaluation, truncated for simplicity. "+" indicates fine-tuned backbones.

experiments are conducted in the re-formulated VQA v2, a response is considered as hitting the format if it includes the option mark like "(A)". Some results are listed in Table 3. It is obvious that the ability is tightly related to the backbone. LVLMs based on raw LLaMA inherit the weak instruction-following ability of the backbone. At the same time, fine-tuning the full backbone results in catastrophic forgetting of the capability, while LoRA-based fine-tuning does not. However, **in-context samples can effectively provide format information and guide LVLMs to respond in the desired format**, facilitating automated evaluation. The complete results are in Table 21.

4.3.4 Generation v.s. Likelihood Evaluation

For generation evaluation, the results reflect the coupling of the multi-modal understanding capability and the instruction-following capability. Meanwhile, likelihood evaluation directly probes the generative models and relaxes the requirement for instruction following.

As shown in Figure 5, likelihood evaluation yields better results than generation evaluation in most cases, even when LVLMs are guided through in-context learning. This indicates that **most LVLMs have limited instruction-following capability, further hindering downstream performance**. We believe the primary factor behind this is the LLM backbone, as models based on FlanT5 and LLama2-Chat have the least performance gap between likelihood and generation evaluation in all the dimensions, FlanT5-based models even perform better using generation evaluation in CG, FG, VGR, and CMI. To address the issue, LVLMs should leverage stronger backbones or introduce sufficiently diverse data for instruct tuning, as done in FlanT5. Besides, the comparison between Vicuna and Vicuna+ demonstrates that **multi-modal instruct tuning the backbone currently can not improve the instruction-following capability of LVLMs**.

4.3.5 Behind the Instability

To investigate the source of instability, we conduct experiments on ScienceQA by applying three types of perturbations separately to LVLMs, including random instructions, shuffling option orders, and random option marks (uppercase, lowercase, or numeric).

Instability Source	Generation	Likelihood
Instruction	0.1607	0.0492
Option Order	0.5523	NA
Option Mark	0.3295	NA

Table 4: Average instability by three types of random perturbations across all models.

As illustrated in Table 4, shuffling the option order results in the highest instability, highlighting a misunderstanding of the option contents. Similar to MMBench (Liu et al., 2023c), we observe that most models exhibit some degree of preference for specific options (refer to Appendix C.6 for more details). Our in-depth finding is that option preference reduces the instability from random instructions and random option marks, but increases the instability from random option orders. The randomness of instruction has the least effect, suggesting that LVLMs can reasonably comprehend the carefully crafted instructions. With likelihood evaluation, the instability is significantly lower because it is a white-box method that directly probes generative models without the need for random sampling during generation. These phenomenons are common

to all models, the complete results are in Appendix C.5. In summary, **current LVLMs are unstable and sensitive to subtle changes in the prompt, especially during black-box evaluations**.

5 CONCLUSION

In this paper, we propose to re-formulate task-oriented multi-modal benchmarks to evaluate LVLMs. By systematically collecting and efficiently re-formulating 61 benchmarks into unified formats that are compatible with LVLMs, we construct a benchmark, ReForm-Eval, which covers 8 capability dimensions. Compared with recently constructed benchmarks for LVLMs, ReForm-Eval provides more data without the need for manual annotation. Additionally, we design dependable automated evaluation methods based on the unified formats, ensuring an impartial assessment of different LVLMs. Leveraging ReForm-Eval, we conduct an exhaustive evaluation of various LVLMs and delve into the factors influencing their performance. Generally, ReForm-Eval serves as a reliable tool for quantitative analysis of LVLMs, aiding in the research and development of LVLMs.

REFERENCES

Harsh Agrawal, Karan Desai, Yufei Wang, Xinlei Chen, Rishabh Jain, Mark Johnson, Dhruv Batra, Devi Parikh, Stefan Lee, and Peter Anderson. Nocaps: Novel object captioning at scale. In *Proceedings of the IEEE/CVF international conference on computer vision*, pp. 8948–8957, 2019.

Firoj Alam, Tanvirul Alam, Md. Arid Hasan, Abul Hasnat, Muhammad Imran, and Ferda Ofli. Medic: A multi-task learning dataset for disaster image classification. *Neural Computing and Applications*, 35:2609–2632, 2023.

Jean-Baptiste Alayrac, Jeff Donahue, Pauline Luc, Antoine Miech, Iain Barr, Yana Hasson, Karel Lenc, Arthur Mensch, Katherine Millican, Malcolm Reynolds, et al. Flamingo: a visual language model for few-shot learning. *Advances in Neural Information Processing Systems*, 35:23716–23736, 2022.

Nitzan Bitton-Guetta, Yonatan Bitton, Jack Hessel, Ludwig Schmidt, Yuval Elovici, Gabriel Stanovsky, and Roy Schwartz. Breaking common sense: Whoops! a vision-and-language benchmark of synthetic and compositional images. *arXiv preprint arXiv:2303.07274*, 2023.

Angel Chang, Angela Dai, Thomas Funkhouser, Maciej Halber, Matthias Niessner, Manolis Savva, Shuran Song, Andy Zeng, and Yinda Zhang. Matterport3d: Learning from rgb-d data in indoor environments. *arXiv preprint arXiv:1709.06158*, 2017.

Keqin Chen, Zhao Zhang, Weili Zeng, Richong Zhang, Feng Zhu, and Rui Zhao. Shikra: Unleashing multimodal llm's referential dialogue magic. *arXiv preprint arXiv:2306.15195*, 2023.

Xinlei Chen, Hao Fang, Tsung-Yi Lin, Ramakrishna Vedantam, Saurabh Gupta, Piotr Dollár, and C Lawrence Zitnick. Microsoft coco captions: Data collection and evaluation server. *arXiv preprint arXiv:1504.00325*, 2015.

Yen-Chun Chen, Linjie Li, Licheng Yu, Ahmed El Kholy, Faisal Ahmed, Zhe Gan, Yu Cheng, and Jingjing Liu. Uniter: Universal image-text representation learning. In *European conference on computer vision*, pp. 104–120. Springer, 2020.

Wei-Lin Chiang, Zhuohan Li, Zi Lin, Ying Sheng, Zhanghao Wu, Hao Zhang, Lianmin Zheng, Siyuan Zhuang, Yonghao Zhuang, Joseph E. Gonzalez, Ion Stoica, and Eric P. Xing. Vicuna: An open-source chatbot impressing gpt-4 with 90%* chatgpt quality, March 2023. URL `https://lmsys.org/blog/2023-03-30-vicuna/`.

Wenliang Dai, Junnan Li, Dongxu Li, Anthony Meng Huat Tiong, Junqi Zhao, Weisheng Wang, Boyang Li, Pascale Fung, and Steven Hoi. Instructblip: Towards general-purpose vision-language models with instruction tuning, 2023.

Abhishek Das, Satwik Kottur, Khushi Gupta, Avi Singh, Deshraj Yadav, José MF Moura, Devi Parikh, and Dhruv Batra. Visual dialog. In *Proceedings of the IEEE conference on computer vision and pattern recognition*, pp. 326–335, 2017.

Jia Deng, Wei Dong, Richard Socher, Li-Jia Li, Kai Li, and Li Fei-Fei. Imagenet: A large-scale hierarchical image database. In *2009 IEEE conference on computer vision and pattern recognition*, pp. 248–255. Ieee, 2009.

Chaoyou Fu, Peixian Chen, Yunhang Shen, Yulei Qin, Mengdan Zhang, Xu Lin, Zhenyu Qiu, Wei Lin, Jinrui Yang, Xiawu Zheng, et al. Mme: A comprehensive evaluation benchmark for multimodal large language models. *arXiv preprint arXiv:2306.13394*, 2023.

Peng Gao, Jiaming Han, Renrui Zhang, Ziyi Lin, Shijie Geng, Aojun Zhou, Wei Zhang, Pan Lu, Conghui He, Xiangyu Yue, et al. Llama-adapter v2: Parameter-efficient visual instruction model. *arXiv preprint arXiv:2304.15010*, 2023.

Rohit Girdhar, Alaaeldin El-Nouby, Zhuang Liu, Mannat Singh, Kalyan Vasudev Alwala, Armand Joulin, and Ishan Misra. Imagebind: One embedding space to bind them all. In *Proceedings of the IEEE/CVF Conference on Computer Vision and Pattern Recognition*, pp. 15180–15190, 2023.

Tao Gong, Chengqi Lyu, Shilong Zhang, Yudong Wang, Miao Zheng, Qian Zhao, Kuikun Liu, Wenwei Zhang, Ping Luo, and Kai Chen. Multimodal-gpt: A vision and language model for dialogue with humans. *arXiv preprint arXiv:2305.04790*, 2023.

Yash Goyal, Tejas Khot, Douglas Summers-Stay, Dhruv Batra, and Devi Parikh. Making the v in vqa matter: Elevating the role of image understanding in visual question answering. In *Proceedings of the IEEE conference on computer vision and pattern recognition*, pp. 6904–6913, 2017.

Danna Gurari, Qing Li, Abigale J Stangl, Anhong Guo, Chi Lin, Kristen Grauman, Jiebo Luo, and Jeffrey P Bigham. Vizwiz grand challenge: Answering visual questions from blind people. In *Proceedings of the IEEE conference on computer vision and pattern recognition*, pp. 3608–3617, 2018.

Jiaming Han, Renrui Zhang, Wenqi Shao, Peng Gao, Peng Xu, Han Xiao, Kaipeng Zhang, Chris Liu, Song Wen, Ziyu Guo, et al. Imagebind-llm: Multi-modality instruction tuning. *arXiv preprint arXiv:2309.03905*, 2023.

Dan Hendrycks, Collin Burns, Steven Basart, Andy Zou, Mantas Mazeika, Dawn Song, and Jacob Steinhardt. Measuring massive multitask language understanding. *arXiv preprint arXiv:2009.03300*, 2020.

Wenbo Hu, Yifan Xu, Y Li, W Li, Z Chen, and Z Tu. Bliva: A simple multimodal llm for better handling of text-rich visual questions. *arXiv preprint arXiv:2308.09936*, 2023.

Yuzhen Huang, Yuzhuo Bai, Zhihao Zhu, Junlei Zhang, Jinghan Zhang, Tangjun Su, Junteng Liu, Chuancheng Lv, Yikai Zhang, Jiayi Lei, et al. C-eval: A multi-level multi-discipline chinese evaluation suite for foundation models. *arXiv preprint arXiv:2305.08322*, 2023.

Zheng Huang, Kai Chen, Jianhua He, Xiang Bai, Dimosthenis Karatzas, Shijian Lu, and CV Jawahar. Icdar2019 competition on scanned receipt ocr and information extraction. In *2019 International Conference on Document Analysis and Recognition (ICDAR)*, pp. 1516–1520. IEEE, 2019.

Drew A Hudson and Christopher D Manning. Gqa: A new dataset for real-world visual reasoning and compositional question answering. In *Proceedings of the IEEE/CVF conference on computer vision and pattern recognition*, pp. 6700–6709, 2019.

Guillaume Jaume, Hazim Kemal Ekenel, and Jean-Philippe Thiran. Funsd: A dataset for form understanding in noisy scanned documents. In *2019 International Conference on Document Analysis and Recognition Workshops (ICDARW)*, volume 2, pp. 1–6. IEEE, 2019.

Justin Johnson, Bharath Hariharan, Laurens Van Der Maaten, Li Fei-Fei, C Lawrence Zitnick, and Ross Girshick. Clevr: A diagnostic dataset for compositional language and elementary visual reasoning. In *Proceedings of the IEEE conference on computer vision and pattern recognition*, pp. 2901–2910, 2017.

Kushal Kafle and Christopher Kanan. An analysis of visual question answering algorithms. In *ICCV*, 2017.

Dimosthenis Karatzas, Lluis Gomez-Bigorda, Anguelos Nicolaou, Suman Ghosh, Andrew Bagdanov, Masakazu Iwamura, Jiri Matas, Lukas Neumann, Vijay Ramaseshan Chandrasekhar, Shijian Lu, et al. Icdar 2015 competition on robust reading. In *2015 13th international conference on document analysis and recognition (ICDAR)*, pp. 1156–1160. IEEE, 2015.

Sahar Kazemzadeh, Vicente Ordonez, Mark Matten, and Tamara Berg. Referitgame: Referring to objects in photographs of natural scenes. In *Proceedings of the 2014 conference on empirical methods in natural language processing (EMNLP)*, pp. 787–798, 2014.

Mahnaz Koupaee and William Yang Wang. Wikihow: A large scale text summarization dataset. *arXiv preprint arXiv:1810.09305*, 2018.

Ranjay Krishna, Yuke Zhu, Oliver Groth, Justin Johnson, Kenji Hata, Joshua Kravitz, Stephanie Chen, Yannis Kalantidis, Li-Jia Li, David A Shamma, et al. Visual genome: Connecting language and vision using crowdsourced dense image annotations. *International journal of computer vision*, 123:32–73, 2017.

Alex Krizhevsky, Geoffrey Hinton, et al. Learning multiple layers of features from tiny images. 2009.

Jianfeng Kuang, Wei Hua, Dingkang Liang, Mingkun Yang, Deqiang Jiang, Bo Ren, and Xiang Bai. Visual information extraction in the wild: practical dataset and end-to-end solution. In *International Conference on Document Analysis and Recognition*, pp. 36–53. Springer, 2023.

Paul Lerner, Olivier Ferret, Camille Guinaudeau, Hervé Le Borgne, Romaric Besançon, José G Moreno, and Jesús Lovón Melgarejo. Viquae, a dataset for knowledge-based visual question answering about named entities. In *Proceedings of the 45th International ACM SIGIR Conference on Research and Development in Information Retrieval*, pp. 3108–3120, 2022.

Juncheng Li, Kaihang Pan, Zhiqi Ge, Minghe Gao, Hanwang Zhang, Wei Ji, Wenqiao Zhang, Tat-Seng Chua, Siliang Tang, and Yueting Zhuang. Empowering vision-language models to follow interleaved vision-language instructions. *arXiv preprint arXiv:2308.04152*, 2023a.

Junnan Li, Dongxu Li, Caiming Xiong, and Steven Hoi. Blip: Bootstrapping language-image pre-training for unified vision-language understanding and generation. In *International Conference on Machine Learning*, pp. 12888–12900. PMLR, 2022.

Junnan Li, Dongxu Li, Silvio Savarese, and Steven Hoi. Blip-2: Bootstrapping language-image pre-training with frozen image encoders and large language models. *arXiv preprint arXiv:2301.12597*, 2023b.

Lei Li, Yuwei Yin, Shicheng Li, Liang Chen, Peiyi Wang, Shuhuai Ren, Mukai Li, Yazheng Yang, Jingjing Xu, Xu Sun, et al. M3it: A large-scale dataset towards multi-modal multilingual instruction tuning. *arXiv preprint arXiv:2306.04387*, 2023c.

Yifan Li, Yifan Du, Kun Zhou, Jinpeng Wang, Wayne Xin Zhao, and Ji-Rong Wen. Evaluating object hallucination in large vision-language models. *arXiv preprint arXiv:2305.10355*, 2023d.

Tsung-Yi Lin, Michael Maire, Serge Belongie, James Hays, Pietro Perona, Deva Ramanan, Piotr Dollár, and C Lawrence Zitnick. Microsoft coco: Common objects in context. In *European conference on computer vision*, pp. 740–755. Springer, 2014.

Fangyu Liu, Guy Emerson, and Nigel Collier. Visual spatial reasoning. *Transactions of the Association for Computational Linguistics*, 11:635–651, 2023a.

Haotian Liu, Chunyuan Li, Qingyang Wu, and Yong Jae Lee. Visual instruction tuning. *arXiv preprint arXiv:2304.08485*, 2023b.

Yuan Liu, Haodong Duan, Yuanhan Zhang, Bo Li, Songyang Zhang, Wangbo Zhao, Yike Yuan, Jiaqi Wang, Conghui He, Ziwei Liu, et al. Mmbench: Is your multi-modal model an all-around player? *arXiv preprint arXiv:2307.06281*, 2023c.

Yuliang Liu, Zhang Li, Hongliang Li, Wenwen Yu, Mingxin Huang, Dezhi Peng, Mingyu Liu, Mingrui Chen, Chunyuan Li, Lianwen Jin, et al. On the hidden mystery of ocr in large multimodal models. *arXiv preprint arXiv:2305.07895*, 2023d.

Pan Lu, Swaroop Mishra, Tanglin Xia, Liang Qiu, Kai-Wei Chang, Song-Chun Zhu, Oyvind Tafjord, Peter Clark, and Ashwin Kalyan. Learn to explain: Multimodal reasoning via thought chains for science question answering. *Advances in Neural Information Processing Systems*, 35:2507–2521, 2022.

Kenneth Marino, Mohammad Rastegari, Ali Farhadi, and Roozbeh Mottaghi. Ok-vqa: A visual question answering benchmark requiring external knowledge. In *Proceedings of the IEEE/cvf conference on computer vision and pattern recognition*, pp. 3195–3204, 2019.

Minesh Mathew, Dimosthenis Karatzas, and CV Jawahar. Docvqa: A dataset for vqa on document images. In *Proceedings of the IEEE/CVF winter conference on applications of computer vision*, pp. 2200–2209, 2021.

Anand Mishra, Karteek Alahari, and CV Jawahar. Top-down and bottom-up cues for scene text recognition. In *2012 IEEE conference on computer vision and pattern recognition*, pp. 2687–2694. IEEE, 2012.

Anand Mishra, Shashank Shekhar, Ajeet Kumar Singh, and Anirban Chakraborty. Ocr-vqa: Visual question answering by reading text in images. In *2019 international conference on document analysis and recognition (ICDAR)*, pp. 947–952. IEEE, 2019.

Maria-Elena Nilsback and Andrew Zisserman. Automated flower classification over a large number of classes. In *Indian Conference on Computer Vision, Graphics and Image Processing*, Dec 2008.

OpenAI. Chatgpt (august 3 version), 2023a. URL `https://chat.openai.com/chat`.

OpenAI. Gpt-4 technical report. *arXiv preprint arXiv:2303.08774*, 2023b.

Omkar M Parkhi, Andrea Vedaldi, Andrew Zisserman, and CV Jawahar. Cats and dogs. In *2012 IEEE conference on computer vision and pattern recognition*, pp. 3498–3505. IEEE, 2012.

Zhiliang Peng, Wenhui Wang, Li Dong, Yaru Hao, Shaohan Huang, Shuming Ma, and Furu Wei. Kosmos-2: Grounding multimodal large language models to the world. *arXiv preprint arXiv:2306.14824*, 2023.

Alec Radford, Jong Wook Kim, Chris Hallacy, Aditya Ramesh, Gabriel Goh, Sandhini Agarwal, Girish Sastry, Amanda Askell, Pamela Mishkin, Jack Clark, et al. Learning transferable visual models from natural language supervision. In *International conference on machine learning*, pp. 8748–8763. PMLR, 2021.

Anhar Risnumawan, Palaiahankote Shivakumara, Chee Seng Chan, and Chew Lim Tan. A robust arbitrary text detection system for natural scene images. *Expert Systems with Applications*, 41 (18):8027–8048, 2014.

Christoph Schuhmann, Richard Vencu, Romain Beaumont, Robert Kaczmarczyk, Clayton Mullis, Aarush Katta, Theo Coombes, Jenia Jitsev, and Aran Komatsuzaki. Laion-400m: Open dataset of clip-filtered 400 million image-text pairs. *arXiv preprint arXiv:2111.02114*, 2021.

Dustin Schwenk, Apoorv Khandelwal, Christopher Clark, Kenneth Marino, and Roozbeh Mottaghi. A-okvqa: A benchmark for visual question answering using world knowledge. arxiv. 2022.

Piyush Sharma, Nan Ding, Sebastian Goodman, and Radu Soricut. Conceptual captions: A cleaned, hypernymed, image alt-text dataset for automatic image captioning. In *Proceedings of the 56th Annual Meeting of the Association for Computational Linguistics (Volume 1: Long Papers)*, pp. 2556–2565, 2018.

Oleksii Sidorov, Ronghang Hu, Marcus Rohrbach, and Amanpreet Singh. Textcaps: a dataset for image captioning with reading comprehension. In *Computer Vision–ECCV 2020: 16th European Conference, Glasgow, UK, August 23–28, 2020, Proceedings, Part II 16*, pp. 742–758. Springer, 2020.

Amanpreet Singh, Vivek Natarajan, Meet Shah, Yu Jiang, Xinlei Chen, Dhruv Batra, Devi Parikh, and Marcus Rohrbach. Towards vqa models that can read. In *Proceedings of the IEEE/CVF conference on computer vision and pattern recognition*, pp. 8317–8326, 2019.

Amanpreet Singh, Guan Pang, Mandy Toh, Jing Huang, Wojciech Galuba, and Tal Hassner. Textocr: Towards large-scale end-to-end reasoning for arbitrary-shaped scene text. In *Proceedings of the IEEE/CVF conference on computer vision and pattern recognition*, pp. 8802–8812, 2021.

Aarohi Srivastava, Abhinav Rastogi, Abhishek Rao, Abu Awal Md Shoeb, Abubakar Abid, Adam Fisch, Adam R Brown, Adam Santoro, Aditya Gupta, Adrià Garriga-Alonso, et al. Beyond the imitation game: Quantifying and extrapolating the capabilities of language models. *arXiv preprint arXiv:2206.04615*, 2022.

Yixuan Su, Tian Lan, Huayang Li, Jialu Xu, Yan Wang, and Deng Cai. Pandagpt: One model to instruction-follow them all. *arXiv preprint arXiv:2305.16355*, 2023.

Quan Sun, Yuxin Fang, Ledell Wu, Xinlong Wang, and Yue Cao. Eva-clip: Improved training techniques for clip at scale. *arXiv preprint arXiv:2303.15389*, 2023.

Tristan Thrush, Ryan Jiang, Max Bartolo, Amanpreet Singh, Adina Williams, Douwe Kiela, and Candace Ross. Winoground: Probing vision and language models for visio-linguistic compositionality. In *Proceedings of the IEEE/CVF Conference on Computer Vision and Pattern Recognition*, pp. 5238–5248, 2022.

Hugo Touvron, Thibaut Lavril, Gautier Izacard, Xavier Martinet, Marie-Anne Lachaux, Timothée Lacroix, Baptiste Rozière, Naman Goyal, Eric Hambro, Faisal Azhar, et al. Llama: Open and efficient foundation language models. *arXiv preprint arXiv:2302.13971*, 2023a.

Hugo Touvron, Louis Martin, Kevin Stone, Peter Albert, Amjad Almahairi, Yasmine Babaei, Nikolay Bashlykov, Soumya Batra, Prajjwal Bhargava, Shruti Bhosale, et al. Llama 2: Open foundation and fine-tuned chat models. *arXiv preprint arXiv:2307.09288*, 2023b.

Maria Tsimpoukelli, Jacob L Menick, Serkan Cabi, SM Eslami, Oriol Vinyals, and Felix Hill. Multimodal few-shot learning with frozen language models. *Advances in Neural Information Processing Systems*, 34:200–212, 2021.

Ramakrishna Vedantam, C Lawrence Zitnick, and Devi Parikh. Cider: Consensus-based image description evaluation. In *Proceedings of the IEEE conference on computer vision and pattern recognition*, pp. 4566–4575, 2015.

Guangzhi Wang, Yixiao Ge, Xiaohan Ding, Mohan Kankanhalli, and Ying Shan. What makes for good visual tokenizers for large language models? *arXiv preprint arXiv:2305.12223*, 2023.

Heming Xia, Qingxiu Dong, Lei Li, Jingjing Xu, Ziwei Qin, and Zhifang Sui. Imagenetvc: Zero-shot visual commonsense evaluation on 1000 imagenet categories. *arXiv preprint arXiv:2305.15028*, 2023.

Ning Xie, Farley Lai, Derek Doran, and Asim Kadav. Visual entailment: A novel task for fine-grained image understanding. *arXiv preprint arXiv:1901.06706*, 2019.

Xudong Xie, Ling Fu, Zhifei Zhang, Zhaowen Wang, and Xiang Bai. Toward understanding wordart: Corner-guided transformer for scene text recognition. In *European Conference on Computer Vision*, pp. 303–321. Springer, 2022.

Peng Xu, Wenqi Shao, Kaipeng Zhang, Peng Gao, Shuo Liu, Meng Lei, Fanqing Meng, Siyuan Huang, Yu Qiao, and Ping Luo. Lvlm-ehub: A comprehensive evaluation benchmark for large vision-language models. *arXiv preprint arXiv:2306.09265*, 2023.

Zhiyang Xu, Ying Shen, and Lifu Huang. Multiinstruct: Improving multi-modal zero-shot learning via instruction tuning. *arXiv preprint arXiv:2212.10773*, 2022.

Barry Menglong Yao, Aditya Shah, Lichao Sun, Jin-Hee Cho, and Lifu Huang. End-to-end multimodal fact-checking and explanation generation: A challenging dataset and models. In *Proceedings of the 46th International ACM SIGIR Conference on Research and Development in Information Retrieval*, pp. 2733–2743, 2023.

Qinghao Ye, Haiyang Xu, Guohai Xu, Jiabo Ye, Ming Yan, Yiyang Zhou, Junyang Wang, Anwen Hu, Pengcheng Shi, Yaya Shi, et al. mplug-owl: Modularization empowers large language models with multimodality. *arXiv preprint arXiv:2304.14178*, 2023.

Zhenfei Yin, Jiong Wang, Jianjian Cao, Zhelun Shi, Dingning Liu, Mukai Li, Lu Sheng, Lei Bai, Xiaoshui Huang, Zhiyong Wang, et al. Lamm: Language-assisted multi-modal instruction-tuning dataset, framework, and benchmark. *arXiv preprint arXiv:2306.06687*, 2023.

Peter Young, Alice Lai, Micah Hodosh, and Julia Hockenmaier. From image descriptions to visual denotations: New similarity metrics for semantic inference over event descriptions. *Transactions of the Association for Computational Linguistics*, 2:67–78, 2014.

Licheng Yu, Patrick Poirson, Shan Yang, Alexander C Berg, and Tamara L Berg. Modeling context in referring expressions. In *Computer Vision–ECCV 2016: 14th European Conference, Amsterdam, The Netherlands, October 11-14, 2016, Proceedings, Part II 14*, pp. 69–85. Springer, 2016.

Rowan Zellers, Yonatan Bisk, Ali Farhadi, and Yejin Choi. From recognition to cognition: Visual commonsense reasoning. In *Proceedings of the IEEE/CVF conference on computer vision and pattern recognition*, pp. 6720–6731, 2019.

Yan Zeng, Hanbo Zhang, Jiani Zheng, Jiangnan Xia, Guoqiang Wei, Yang Wei, Yuchen Zhang, and Tao Kong. What matters in training a gpt4-style language model with multimodal inputs? *arXiv preprint arXiv:2307.02469*, 2023.

Pengchuan Zhang, Xiujun Li, Xiaowei Hu, Jianwei Yang, Lei Zhang, Lijuan Wang, Yejin Choi, and Jianfeng Gao. Vinvl: Revisiting visual representations in vision-language models. In *Proceedings of the IEEE/CVF Conference on Computer Vision and Pattern Recognition*, pp. 5579–5588, 2021.

Yunqing Zhao, Tianyu Pang, Chao Du, Xiao Yang, Chongxuan Li, Ngai-Man Cheung, and Min Lin. On evaluating adversarial robustness of large vision-language models. *arXiv preprint arXiv:2305.16934*, 2023.

Deyao Zhu, Jun Chen, Xiaoqian Shen, Xiang Li, and Mohamed Elhoseiny. Minigpt-4: Enhancing vision-language understanding with advanced large language models. *arXiv preprint arXiv:2304.10592*, 2023.

A Benchmark Construction

In this section, we introduce the collected datasets and the corresponding re-formulation procedures in detail. The statistics of the re-formulated datasets are provided in Table 5 and Table 6.

A.1 Coarse-Grained Perception

For the Flowers102 dataset, we employ the complete validation set for evaluation purposes. However, for CIFAR10, ImageNet-1K, Pets37, and VizWiz, we perform random subsampling of 10%. Concerning the TDIUC dataset, given that certain models in their training phase utilized a portion of the TDIUC dataset originating from the Visual Genome, we initially exclude this subset of data to prevent potential data leakage. Subsequently, we apply a shuffling operation to the entire TDIUC dataset and perform equidistant sampling, resulting in the selection of 2.5% of the sport_recognition data ($\text{TDIUC}_{\text{sport}}$) and 1% of the scene_recognition data ($\text{TDIUC}_{\text{scene}}$). In the case of MEDIC(Alam et al., 2023), we sample an equal number of samples from each label to balance the answer distribution.

For Flowers102 and Pets37, we randomly select three incorrect class labels, in addition to the correct label, from their original set of categories to form multiple-choice question options. For the TDIUC, we aggregate all answers for the same task to create an answer pool, and then utilize the same approach above to construct four answer options for multiple-choice questions.

For ImageNet-1K, we calculate similarities within its own set of 1000 categories using WordNet and selected the four options with the highest similarity to the correct class as choices (the highest one must be the right answer, and we need to get them out of order).

For CIFAR10, we initially employ WordNet to identify synonyms of the answers that are semantically related but not synonymous. These synonyms are then ranked based on their similarity. Subsequently, we manually adjust some of the less common candidate options. Finally, we likewise select the top four options with the highest similarity as all choices.

As for VizWiz, we re-formulate it into two benchmarks: VizWiz_2 as a binary classification task to determine whether there is any quality issue with the image. VizWiz_4 as a 4-choice question, requiring the model to determine the exact reason for the quality issue. We sort the issues related to image quality based on the number of votes in the annotations, the top one is considered the true label while the second to fourth options serve as negative choices.

For MEDIC (Alam et al., 2023), it is re-formulated to $\text{MEDIC}_{\text{dts}}$, a benchmark for disaster type selection (dts), we directly use all seven classification labels as choice options.

A.2 Fine-Grained Perception

For TDIUC (Kafle & Kanan, 2017), we initially exclude the subset sourced from Visual Genome (Krishna et al., 2017) to prevent evaluation on the training data. Then, we shuffle the entire dataset and conducted an equidistant sampling strategy for task sample balance. Specifically, we sample 1% of the data for color ($\text{TDIUC}_{\text{color}}$), detection($\text{TDIUC}_{\text{detection}}$), and counting tasks ($\text{TDIUC}_{\text{counting}}$), and 2.5% for position tasks. As for the utility task ($\text{TDIUC}_{\text{utility}}$), we retain and utilized all 171 data samples. For answer options, we uniformly count all answers within the data and randomly selected three options other than the correct answer to form all four choices.

Regarding RefCOCO (Yu et al., 2016), we re-formulate the referring expression selection ($\text{RefCOCO}_{\text{res}}$) task, in which the LVLMs are supposed to select the correct referring expression from the options based on the image region in the bounding box. We sample an equal number of samples from each object category, in order to balance the correct referring expression categories appearing in the questions. As for negative options in each question, we sample the negative referring expression from a distinct subcategory within the same category as the positive sample.

For MSCOCO (Lin et al., 2014), we re-formulate four tasks: object counting (counting), multiple class identification ($\text{MSCOCO}_{\text{mci}}$), grounded object identification ($\text{MSCOCO}_{\text{goi}}$) and missing object selection ($\text{MSCOCO}_{\text{mos}}$) for object-level evaluation. The multiple class identification task aims to evaluate the LVLM's ability of object classification. Further, the grounded object identification and missing object selection tasks concentrate on object perception within a specified region of interest.

Task Name	Dataset Name	Data Source	Datset Split	# of Images	# of Samples
Coarse-grained Perception	Flowers102	Flowers102	val	818	818
	CIFAR10	CIFAR10	test	10000	10000
	ImageNet-1K	ImageNet-1K	val	50000	50000
	Pets37	Pets37	test	3669	3669
	VizWiz_2	VizWiz	val	4049	4049
	VizWiz_4	VizWiz	val	2167	2167
	$\text{TDIUC}_{\text{sport}}$	TDIUC	val	6001	8696
	$\text{TDIUC}_{\text{scene}}$	TDIUC	val	9219	21320
	$\text{MEDIC}_{\text{dts}}$	MEDIC	test	15688	15688
Fine-grained Perception	$\text{MSCOCO}_{\text{mci}}$	MSCOCO	val2017	2323	3600
	$\text{MSCOCO}_{\text{goi}}$	MSCOCO	val2017	2404	3600
	$\text{MSCOCO}_{\text{mos}}$	MSCOCO	val2017	2479	2479
	$\text{TDIUC}_{\text{color}}$	TDIUC	val	18808	38267
	$\text{TDIUC}_{\text{utility}}$	TDIUC	val	162	171
	$\text{TDIUC}_{\text{postiion}}$	TDIUC	val	7131	9247
	$\text{TDIUC}_{\text{detection}}$	TDIUC	val	21845	29122
	$\text{TDIUC}_{\text{counting}}$	TDIUC	val	26166	41991
	$\text{RefCOCO}_{\text{res}}$	RefCOCO	val	9397	34540
	$\text{MSCOCO}_{\text{count}}$	MSCOCO	val2014	513	513
Scene Text Perception	CUTE80	CUTE80	all	288	288
	IC15	IC15	test	1811	1811
	IIIT5K	IIIT5K	test	3000	3000
	COCO-Text	COCO-Text	val	9896	9896
	WordArt	WordArt	test	1511	1511
	TextOCR	TextOCR	val	3000	3000
	Grounded IC15	IC15	val	221	849
	Grounded COCO-Text	COCO-Text	val	1574	3000
	Grounded TextOCR	TextOCR	val	254	3000
	FUNSD	FUNSD	test	47	588
	POIE	POIE	test	750	6321
	SROIE	SROIE	test	347	1388
	TextVQA	TextVQA	val	3023	4508
	DocVQA	DocVQA	val	1286	5312
	OCR-VQA	OCR-VQA	test	3768	3944

Table 5: Dataset statistics of visual perception tasks in ReForm-Eval.

The former allows models to assess which object exists within the given bounding box of the image, while the latter asks models to judge which object disappears within all the given bounding boxes of the image.

For the multiple class identification and grounded object identification tasks, we randomly sample 300 object annotations from each super-category in the valid split to ensure balance. This results in a total of 3600 evaluation data samples for each task. For the mos task, we filter out the objects with the height and width of their bounding boxes smaller than 50 and finally get 2479 samples. As for options generation, we employ a hierarchical strategy. For the multiple class identification task, we begin by randomly selecting the object class from within the super-category of the target object. If there are insufficient options, we broaden our selection to all object categories. In tasks related to region, our initial step is to randomly choose object categories present in the image but do not meet the requirement specified in the question. In cases where this is not possible, we follow the sampling procedure used in the multiple-class identification task. The examples of these grounded fine-grained tasks as shown in Table 6. The counting task has the same setting as the counting task in the TDIUC dataset.

A.3 Scene Text Perception

For OCR, we use 6 original OCR benchmarks (including CUTE80 (Risnumawan et al., 2014), IC15 (Karatzas et al., 2015), IIIT5K (Mishra et al., 2012), COCO-Text (Mishra et al., 2012), WordArt (Xie et al., 2022) and TextOCR (Singh et al., 2021)) as the evaluation tasks. Current OCR

Task Name	Dataset Name	Data Source	Datset Split	# of Images	# of Samples
Spatial Understanding	CLEVR	CLEVR	val	5726	6900
	VSR	VSR	test	1074	1811
	MP3D-Spatial	MP3D	-	3341	4735
Cross-Modal Inference	COCO_{itm}	MSCOCO caption	val2017	5000	25014
	COCO_{its}	MSCOCO caption	val2017	5000	25014
	WikiHow	WikiHow	val	32194	32194
	Winoground	Winoground	all	800	800
	SNLI-VE	SNLI-VE	test	1000	17901
	MOCHEG	MOCHEG	test	1452	3385
Visually Grounded Reasoning	VQA v2	VQA v2	val2014	15638	21441
	GQA	GQA	testdev	398	12578
	Whoops	Whoops	all	498	3362
	OK-VQA	OK-VQA	val	5032	5045
	ScienceQA	ScienceQA	test	2017	2017
	VizWiz	VizWiz	val	4319	4319
	ViQuAE	ViQuAE	test	1105	1257
	K-ViQuAE	ViQuAE	test	1094	1245
	A-OKVQA	A-OKVQA	val	1122	1145
	A-OKVQRA	A-OKVQA	val	1122	1145
	A-OKVQAR	A-OKVQA	val	1122	1145
	ImageNetVC	ImageNetVC	all	3916	4076
Multi-Turn Dialogue	VQA-MT	VQA v2	val2014	1073	1073
	VisDial	VisDial	val2018	2064	2064
Visual Description	COCO	MSCOCO caption	val2017	5000	5000
	TextCaps	TextCaps	val	3166	3166
	NoCaps	NoCaps	val	4500	4500
	Flickr30K	Flickr30K	test	1000	1000

Table 6: Dataset statistics of visual cognition tasks in ReForm-Eval.

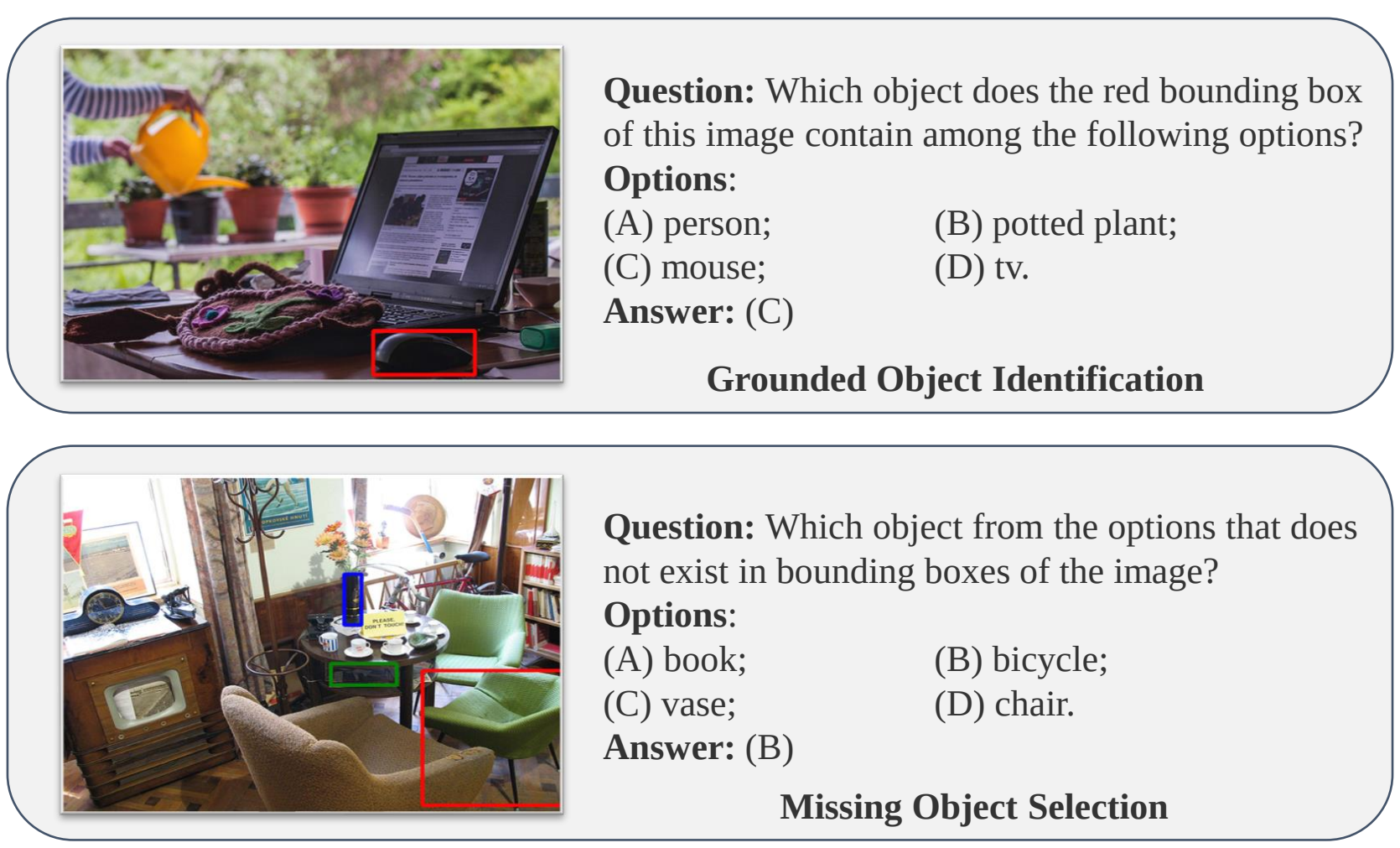

Figure 6: Examples of grounded fine-grained tasks.

benchmarks utilize cropped images containing only target text as visual input sources (Xu et al., 2023; Liu et al., 2023d). To further assess text identification in complex visual contexts, we propose grounded OCR tasks (including gIC15, gCOCO-Text, and gTextOCR). Specifically, we filter out the bounding boxes containing target texts larger than 40x40 for better evaluation. The image, along with the bounding box annotations and the corresponding instruction, will be fed into the model for evaluation, which is similar to the grounded fine-grained tasks (i.e. $\text{MSCOCO}_{\text{goi}}$).

For KIE, we utilize the test splits of 3 benchmarks (including SROIE (Huang et al., 2019), POIE (Kuang et al., 2023) and FUNSD (Jaume et al., 2019)) as the evaluation tasks.

And for OCR-based VQA, we use 3 benchmarks (including TextVQA (Singh et al., 2019), DocVQA (Mathew et al., 2021) and OCR-VQA (Mishra et al., 2019)) as the evaluation tasks. We filter out the question-answer pairs that need to be inferred based on the scene texts.

A.4 Visually Grounded Reasoning

For VQAv2 (Goyal et al., 2017), we sample 10% for reformulation owing to the extremely large population. Besides, since ViQuAE (Lerner et al., 2022) provides relevant knowledge information for each question, we additionally construct K-ViQuAE with knowledge as context, which assesses models' reasoning ability hierarchically with ViQuAE (Lerner et al., 2022). For ScienceQA (Lu et al., 2022), only 2017 questions of all the 4241 test set are paired with an image, which are selected in our benchmark. Besides, original A-OKVQA (Schwenk et al., 2022) gives rationales for answering each question, therefore we construct A-OKVQRA and A-OKVQAR for hierarchical evaluation.

For VQAv2 (Goyal et al., 2017), GQA (Hudson & Manning, 2019), OK-VQA (Marino et al., 2019), VizWiz (Gurari et al., 2018), ViQuAE (Lerner et al., 2022) and Whoops (Bitton-Guetta et al., 2023), ChatGPT is employed to generate appropriate negative options, and the prompt template for querying is:

> You are a multiple-choice generator. Given a question and an answer, you need to generate three additional incorrect options while ensuring their plausibility and confusion.
> Question: {question}
> Answer: {correct answer}

Note that for yes or no questions, the negative option is directly derived as no or yes, and ChatGPT is not employed.

While ImageNetVC (Xia et al., 2023) randomly selects 3 candidate options from the correspondent answer set with the commonsense type of each question. As for ScienceQA (Lu et al., 2022) and A-OKVQA (Schwenk et al., 2022), they adopt their original options because of the original single-choice formulation.

As for A-OKVQAR, the prompt template for querying ChatGPT to generate negative rationales is:

> You are a multiple-choice generator. Given a question and an answer, along with a rationale for that answer, you need to generate 3 counterfactual rationales. These counterfactual rationales should be contextually relevant while also being sufficiently distinct from the correct rationale.
> Question: {question}
> Answer: {correct answer}
> Rationale: {rationale}

A.5 Spatial Understanding

For CLEVR (Johnson et al., 2017), we filter out the question types that do not involve spatial relations and randomly select 300 samples from each question type related to spatial relations. For different question types, we randomly select false options from their corresponding answer sets. In cases where some question types have insufficient options, we add 'Not sure' and 'Unknown' as false options to maintain the number of four options.

For VSR (Liu et al., 2023a), the original dataset comprises captions that describe true or false spatial relations among objects in the corresponding images. We select image-caption pairs from the test split where the spatial descriptions are right and use them for our evaluation tasks. The false options are generated by randomly sampling different spatial relations from the test split.

MP3D (Chang et al., 2017) also known as Matterport3D, comprises a large-scale collection of RGB-D images captured from nearly 10,800 real indoor viewpoints with 50,811 object instance annotations. Based on this dataset, we extract two types of spatial relations to re-formulate our benchmark MP3D-Spatial: object-object level relations (left, right, above, under, on top of, and next to) and object-observer level relations (far and close). For spatial relations 'on top of' and 'next to,' we use

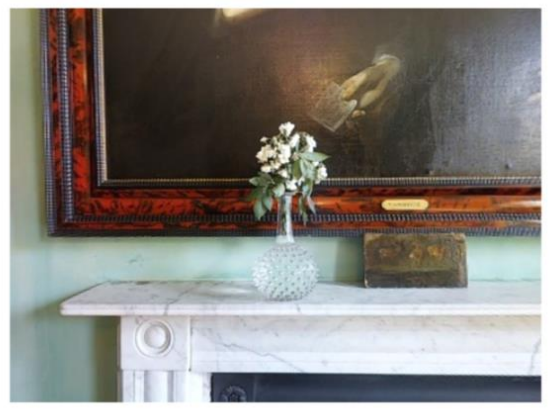

Question: Describe the spatial connection between vase and mantel within the image.
Options:
(A) The vase is inside the mantel;
(B) The vase is right of the mantel;
(C) The vase is next to the mantel;
(D) The vase is on the top of the mantel.
Answer: (D)

Question: In the image, point out the object that has the greatest distance from you.
Options:
(A) picture;
(B) refrigerator;
(C) stairs;
(D) unknown.
Answer: (B)

Figure 7: Examples of spatial relation judgment in MP3D-Spatial.

1,135 annotated samples for our task. For other relations, we utilize both bounding box information and depth to determine the spatial relationships and extract 600 samples for each type of relation. As for false options, we randomly select non-matching spatial relations to serve as the incorrect options for our reformulated task. The examples of the re-formulated data are shown in Figure 7

A.6 Cross-Modal Inference

In this section, we consider two kinds of tasks, including image text matching and visual entailment.

For MSCOCO (Lin et al., 2014), we re-formulate two tasks, including COCO image text matching (COCO_{itm}) and COCO image text selection (COCO_{its}). The matching task requests LVLMs to determine whether the given image and text are matched. The selection task instructs LVLMs to select the best-matched caption for the given image. We randomly sample image and text pairs as positive samples. For each image, we first find the negative images that have distinct but similar object categories. For each negative image, we find the most similar captions with the positive caption according to the object appearing in the sentence.

WikiHow (Koupaee & Wang, 2018) provides introductions to common skills. Within each skill, there are multiple crucial tasks, and each task is composed of several steps. We re-formulate the Wikihow image text selection task, in which given the task name, the LVLMs are supposed to choose the matching step description. We randomly sample visual and textual descriptions of the steps to form multiple-choice questions. To mine the hard negative options, we try to randomly take three samples from the same task as the positive sample. If the negative samples from the task level are insufficient, we then select some from the skill level and dataset level in turn.

For Winoground (Thrush et al., 2022), we re-formulate a caption selection task, which requires models to choose the correct caption. Since Winoground has captions for each image pair that have exactly the same words but in a different order, the options are the captions for every image pair.

For SNLI-VE (Xie et al., 2019), we re-formulate the visual entailment task, in which the LVLMs are required to determine whether the text can be inferred based on the image clues and should give answer of uncertainty when the evidence is insufficient. The options of multiple-choice question comprise “yes”, “not sure” and “no”. To balance the correct answer distribution, for each image, we sample an equal number of samples from each label.

For MOCHEG (Yao et al., 2023), we re-formulate the visual and textual entailment task, in which the LVLMs are supposed to determine whether the claim can be infered based on the visual and textual evidence and judge out whether the evidences are insufficient. The options consist of “supported”, “refuted” and “not enough information”.

A.7 Visual Description

We re-formulate the image captioning task from four dataset including MSCOCO (Lin et al., 2014), TextCaps (Sidorov et al., 2020), NoCaps (Agrawal et al., 2019) and Flickr30K (Young et al., 2014).

In this task, the LVLMs are expected to generate a brief description for given image. Among these dataset, TextCaps additionally examines the optical character recognition capability of LVLMs by requesting models to pointing out the text in the image. We randomly sample these datasets for evaluation.

A.8 Multi-Turn Dialogue

To mimic a naive setup, we construct VQA-MT (VQA Multi-Turn) by considering multiple questions for the same image and gathering them into a multi-turn conversation. For VQA-MT, different images are accompanied by different amounts of questions in the re-formulated VQA v2 (Goyal et al., 2017), only the images with more than 2 questions are kept. For images with more than 10 questions, only the first 10 questions are kept. All questions for the same image are arranged into a dialogue without inter-round dependencies. In the filtered dataset, there are 1073 image-dialogue pairs. The negative options are directly adopted from the re-formulated VQA v2.

As for VisDial (Das et al., 2017), there is a 10-turn QA dialogue for each image. the original datasets provide 100 options for each question while. The prompt template for querying GPT-3.5 to generate negative options is:

> I will provide a question with the correct answer, please give me 3 incorrect options to help me get a single-choice question.
> Question: {question}
> Answer: {correct answer}

Different from the original VisDial to perform offline dialogue (the history contains correct answers), we perform online dialogue (the history contains the previous output of the models). To further investigate whether the performance of LVLMs changes with an increasing number of dialogue turns, we calculate the correlation coefficient between the accuracy and the number of dialogue turns.

B Evaluation Details

B.1 Implementation Details

Our benchmark and the evaluation framework are PyTorch-based. All experiments are conducted on 8 Tesla V100 GPUs. During the evaluation, half precision is used to accelerate the process.

To ensure fair comparisons between LVLMs, we try our best to keep the parameter setting aligned with the demo code provided by the original codebase. However, we limit the maximum number of tokens a model can generate for all LVLMs. It is set to 30 for most questions except the image-caption task where it is set to the upper quartile (the 75th percentile) of the reference caption length in the corresponding datasets. all input texts are formulated into conversations as required by different models, using the same system messages, roles, and separators. As for the image input, we only consider single-image inputs, we use the same preprocess method mentioned in the original paper except for Lynx, which utilizes 420×420 input resolution and we still use 224×224 for a fair comparison.

It is worth noting that ReForm-Eval comprises a total of over 500,000 evaluation instances across over 300,000 images, and considering the need for multiple tests for each instance, this results in significant computational cost. To this end, we further construct a subset by sub-sampling 10% data from the whole ReForm-Eval. All experiments conducted in this paper are based on the subset. We will open-source both the subset we use and the complete data for the research community.

B.2 Models

In this section, we introduce the evaluated LVLMs in detail. For each method, we identify the version assessed in this paper if multiple variants are provided by the method. Additionally, we summarize the architecture of LVLMs in Table 7 and the datasets they use in Table 8.

Model	Model Architecture					
	Vis Encoder	LLM	Connection Module	#oP	#oTP	#oVT
BLIP-2	ViT-G/14	FlanT5-XL	Q-Former	3.94B	106.7M	32
InstructBLIP$_F$	ViT-G/14	FlanT5-XL	Q-Former	4.02B	187.2M	32
InstructBLIP$_V$	ViT-G/14	Vicuna-7B	Q-Former	7.92B	188.8M	32
LLaVA$_V$	ViT-L/14	Vicuna-7B	Linear	7.05B	6.74B	256
LLaVA$_{L_2}$	ViT-L/14	LLaMA2-7B	Linear	7.05B	6.74B	256
MiniGPT4	ViT-G/14	Vicuna-7B	Q-Former+Linear	7.83B	3.1M	32
mPLUG-Owl	ViT-L/14	LLaMA-7B	Perceiver	7.12B	384.6M	65
PandaGPT	ImageBind	Vicuna-7B+LoRA	Linear	7.98B	37.8M	1
IB-LLM	ImageBind	LLaMA-7B+LoRA+BT	BindNet+Gate	8.61B	649.7M	1
LA-V2	ViT-L/14	LLaMA-7B+BT	Linear+Adapter+Gate	7.14B	63.1M	10
mmGPT	ViT-L/14	LLaMA-7B+LoRA	Perceiver+Gate	8.37B	23.5M	64
Shikra	ViT-L/14	Vicuna-7B	Linear	6.74B	6.44B	256
Lynx	ViT-G/14	Vicuna-7B+Adapter	Perceiver	8.41B	688.4M	64
Cheetor$_V$	ViT-G/14	Vicuna-7B	Query+Linear+Q-Former	7.84B	6.3M	32
Cheetor$_{L_2}$	ViT-G/14	LLaMA2-Chat	Query+Linear+Q-Former	7.84B	6.3M	32
BLIVA	ViT-G/14	Vicuna-7B	Q-Former+Linear	7.92B	194.6M	32

PS: Underlined represents a trainable component. "BT" represents bias-tuning . "BindNet" represents bind network.

Table 7: Model architecture of different LVLMs. "#oP", "#oTP", and "#oVT" are number of total parameters, number of trainable parameters, and number of visual tokens, respectively.

BLIP-2 BLIP-2 (Li et al., 2023b) is pre-trained in two stages: the representation learning stage and the generative learning stage, where the image encoder and the LLM are frozen and only a lightweight Q-Former is trained for bridging the modality gap. "blip2-pretrain-flant5xl" is evaluated in our experiment.

InstructBLIP InstructBLIP (Dai et al., 2023) further extends BLIP-2 with task-oriented instruct tuning, pre-trained with Vicuna using the same procedure as BLIP-2. Additionally, an instruction-aware Q-Former module is proposed in InsturctBLIP, which takes in the instruction text tokens as additional input to the Q-Former. During instruction tuning, only parameters of Q-Former are fine-tuned based on pre-trained checkpoints, while keeping both the image encoder and the LLM frozen. We take "blip2-instruct-vicuna7b" and "blip2-instruct-flant5xl" as evaluation versions.

MiniGPT-4 MiniGPT4 (Zhu et al., 2023) adds a trainable single projection layer based on BLIP-2 and also adopts a two-stage training approach, where the first stage is pre-training the model on large aligned image-text pairs and the second stage is instruction tuning with a smaller but high-quality image-text dataset with a designed conversational template. During training, the image encoder, the LLM, and the Q-Former are all frozen. "pretrained-minigpt4-7b" is used in our setup.

LLaVA LLaVA (Liu et al., 2023b) employs a linear layer to convert visual features into the language embedding space, with a pre-training and instruction tuning stage. During pre-training, both the visual encoder and LLM weights were frozen. Then, keeping only the visual encoder weights frozen, the weights of the projection layer and LLM in LLaVA are updated with generated instruction data. In our experiment, "liuhaotian/LLaVA-7b-delta-v0" and "liuhaotian/llava-llama-2-7b-chat-lightning-lora-preview" are used for evaluation.

mPLUG-Owl mPLUG-Owl (Ye et al., 2023) proposes a novel training paradigm with a two-stage fashion. During pre-training, mPLUG-Owl incorporates a trainable visual encoder and a visual abstractor, while maintaining the LLM frozen. In the stage of instruction tuning, language-only and multi-modal instruction data are used to fine-tune a LoRA module on the LLM. "MAGAer13/mplug-owl-llama-7b" is used in our experiment, but LoRA is not implemented in this version.

ImageBind-LLM (IB-LLM) ImageBind-LLM (Han et al., 2023) adopts a two-stage training pipeline. In the pre-training stage, a learnable bind network and a gating factor are updated. The bind network transforms image features, while the gating factor weights the transformed image features to determine the magnitude of injecting visual semantics and the result is added to each word token for each layer. In the instruction tuning stage, a mixture of language instruction data and visual

Model	Pre-training Data		Instruction Data	
	Dataset	Size	Dataset	Size
BLIP-2	MSCOCO+VG+CC3M+ CC12M+SBU+L400M	129M	-	-
InstructBLIP	Following BLIP-2	129M	COCO Caption+ WebCapFilt+ TextCaps+VQAv2+ OKVQA+A-OKVQA+ OCR-VQA+LLaVA	16M
LLaVA	CC3M	595K	LLaVA	158K
MiniGPT4	CC3M+SBU+L400M	5M	CC3M formatted by ChatGPT	3.5K
mPLUG-Owl	L400M+COYO+ CC3M+MSCOCO	104B tokens	Alpaca+Vicuna+ Baize+LLaVA	102K+90K+ 50K+158K
PandaGPT	-	-	MiniGPT4+LLaVA	160K
IB-LLM	CC3M+SBU+L2B+ COYO+MMC4	940M	Alpaca+GPT4LLM+ ShareGPT+ MiniGPT4+LLaVA	NA
LA-V2	COCO Caption	567K	GPT4LLM	52K
mmGPT	-	-	Dolly15K+GPT4LLM+ LLaVA+MiniGPT4+ A-OKVQA+ COCO Caption+ OCR VQA formatted by ChatGPT	15K+52K+ 158K+3.5K 5K+0.5K+0.5K
Shikra	LLaVA-Pretraining+ Flickr30K+ VG+RefCOCO+ VQAv2+PointQA+ Visual7W+VCR	$\sim$ 4.3M	LLaVA+Shikra-RD	158K+5.9K
Lynx	BlipCapFilt+ CC12M+CC3M+SBU+ more 26 datasets (listed in Table 9 in Lynx)	14B tokens	text-only+image-text+ video-text data (all 32 datasets are listed in Table 9 in Lynx)	3B tokens
Cheetor	pre-training image-text data	5M	CAGIT+image-text data	64K+700K
BLIVA	L400M+CC3M+ SBU	558K	Following InstructBLIP	$\sim$ 2.4M

Table 8: Pre-training data and instruction tuning data used by different LVLMs. In Lynx, the training data size is represented by "tokens" and these tokens are considered as consumed samples rather than data volume, which is also the case for the pre-training data in mPLUG-Owl. "L400M" and "L2B" refer to LAION-400M and LAION-2B, repectively. GPT4LLM is a GPT4 version of Alpaca with higher quality. "$\sim$" denotes that the value is approximated by multiplying the batch size with the training steps of one epoch. "NA" denotes that the specific size is not mentioned in the corresponding paper.

instruction data is used to update partial parameters in LLaMA by LoRA and bias-norm tuning. We utilize "Cxxs/ImageBind-LLM/7B" for evaluation and call it "IB-LLM".

LLaMA-Adapter V2 In LLaMA-Adapter V2 (Gao et al., 2023), a joint training paradigm is proposed, where only the visual projection layers and early zero-initialized attention with gating are pre-trained using image-text data, while the late adaptation prompts with zero gating, the unfrozen norm, newly added bias, and scale factors are implemented for learning from the language-only instruction data. "LLaMA-Adapter-V2-BIAS-7B" is applied for evaluation.

Multimodal-GPT (mmGPT) Multimodal-GPT (Gong et al., 2023) is fine-tuned from Open-Flamingo, where the whole open-flamingo model is frozen and the LoRA module is added and updated to the self-attention, cross-attention, and FFN part in the LLM, using language-only and multimodal instruction data. “mmgpt-lora-v0-release” is used for evaluation. To simplify, we refer to it as “mmGPT”.

PandaGPT PandaGPT (Su et al., 2023) utilizes a one-stage training method using a combination of 160k image-language instruction-following data from MiniGPT-4 and LLaVA, where only two components are trained: a linear projection matrix connecting the visual representation generated by ImageBind to Vicuna, and additional LoRA weights applied to Vicuna attention modules. “openllmplayground/pandagpt-7b-max-len-1024” is evaluated as our implemented version.

Shikra Shikra (Chen et al., 2023) consists of a vision encoder, an alignment layer, and an LLM. This model is trained in two stages, where both the fully connected layer and the entire LLM are trained and the visual encoder is frozen. We select “shikras/shikra-7b-delta-v1” for our evaluation in this experiment.

Cheetor Cheetor (Li et al., 2023a) is initialized from BLIP-2 and pre-trains Q-Former that matches Vicuna and LLaMA2. A lightweight CLORI module is introduced that leverages the sophisticated reasoning ability of LLMs to control the Q-Former to conditionally extract specific visual features, and further re-inject them into the LLM. During training, only a set of query embeddings and two linear projection layers need to be updated. “cheetah-llama2-7b” and “cheetah-vicuna-7b” are specifically used for assessment.

Lynx Lynx (Zeng et al., 2023) leverages the method of pre-training and instruction tuning, where lightweight trainable adapters are added after some layers in the frozen LLMs and a resampler mechanism is adapted to reduce the vision token sequence, using learnable latent queries. During pre-training, the newly added layers are trained to build connections of different modalities. “finetune-lynx” is opted for evaluation.

BLIVA BLIVA (Hu et al., 2023) is initialized from a pre-trained InstructBLIP and merges learned query embeddings output by the Q-Former with projected encoded patch embeddings. Demonstrating a two-stage training paradigm, the patch embeddings projection layer is pre-trained and both the Q-Former and the project layer are fine-tuned by instruction tuning data. “mlpc-lab/BLIVA-Vicuna” is employed under evaluation in our experiment.

C Complementary Results and Analysis

C.1 Per-Dimension Results and Analysis

In this section, we will provide the complete results and corresponding analysis of all capability dimensions.

C.1.1 Results on Coarse-grained Perception

Tabel 9 and Table 10 provide results of coarse-grained perception tasks, including image classification and scene recognition. For generation evaluation, BLIP-2 and InstructBLIP take the lead in most tasks except the image quality assessment in VizWiz. We speculate that this is because the training data primarily consists of text describing the visual content, with very little description of the image quality, which may result in models not understanding the image quality. However, this challenge is also faced by most LVLMs, some of them act worse than random guesses.

For likelihood evaluation, the situation is slightly different. Most models perform better across different datasets while BLIP-2 and InstructBLIP struggle in Flowers102, ImageNet-1K, Pets37, and MEDIC. We hypothesize this is due to the fact that the category names of these datasets are not common, the calculated likelihood may not be as effective as those for common tokens. As mentioned in Section C.4, the diversity of the pre-training data used by BLIP-2 and InstructBLIP is limited, while mPLUG-Owl utilizes diverse pre-training data. This explains why mPLUG-Owl

Model	Image Classification											
	Flowers102		CIFAR10		ImageNet-1K		Pets37		$VizWiz_4$		$VizWiz_2$	
	Acc	Instby	Acc	Instby	Acc	Instby	Acc	Instby	Acc	Instby	Acc	Instby
Generation Evaluation												
BLIP-2_F	75.57	0.07	**87.32**	0.03	73.07	0.11	75.19	0.06	24.44	0.25	46.68	0.00
$InstructBLIP_F$	**77.75**	0.04	83.72	0.02	**77.06**	0.07	**83.28**	0.02	27.59	0.15	47.43	0.01
$InstructBLIP_V$	72.81	0.06	86.28	0.03	71.78	0.06	80.77	0.06	**48.00**	0.05	49.37	0.41
$LLaVA_V$	35.92	0.45	14.38	0.69	19.48	0.60	25.90	0.20	14.91	0.93	45.20	0.43
$LLaVA_{L_2}$	50.07	0.23	41.42	0.21	50.74	0.15	41.42	0.21	27.31	0.28	46.44	0.02
MiniGPT4	43.89	0.20	43.06	0.44	48.85	0.31	43.06	0.44	31.30	0.39	45.89	0.27
mPLUG-Owl	37.56	0.52	37.30	0.29	37.54	0.30	42.19	0.41	31.85	0.75	46.09	0.49
PandaGPT	34.43	0.61	26.32	0.06	27.63	0.05	29.07	0.02	31.11	0.31	29.75	0.84
IB-LLM	26.99	0.13	23.42	0.00	22.45	0.12	24.59	0.48	26.02	0.29	49.90	0.24
LA-V2	25.89	0.44	25.96	0.42	18.08	0.64	29.07	0.02	33.05	0.29	54.21	0.03
mmGPT	26.21	0.64	25.92	0.27	25.60	0.25	27.48	0.25	28.24	0.69	50.59	0.32
Shikra	41.54	0.11	50.72	0.11	47.99	0.10	42.62	0.11	21.48	0.21	47.72	0.13
Lynx	56.19	0.30	77.20	0.11	57.82	0.26	60.98	0.32	26.30	0.19	**54.60**	0.01
$Cheetor_V$	55.26	0.27	59.12	0.11	46.51	0.25	44.86	0.28	33.98	0.23	49.90	0.16
$Cheetor_{L_2}$	37.80	0.23	70.82	0.15	43.64	0.15	36.39	0.21	31.11	0.24	46.88	0.06
BLIVA	30.71	0.22	37.52	0.21	36.68	0.20	35.57	0.25	32.78	0.19	48.71	0.20
Likelihood Evaluation												
BLIP-2_F	56.31	0.05	89.40	0.03	51.40	0.07	54.10	0.07	12.78	0.01	48.12	0.04
$InstructBLIP_F$	55.23	0.04	81.62	0.02	53.32	0.06	56.34	0.05	12.96	0.03	49.45	0.05
$InstructBLIP_V$	50.44	0.04	88.40	0.03	44.04	0.06	51.20	0.06	14.91	0.02	51.09	0.08
$LLaVA_V$	48.78	0.04	92.56	0.01	51.16	0.05	47.98	0.05	14.35	0.00	54.21	0.06
$LLaVA_{L_2}$	48.51	0.04	48.52	0.06	42.12	0.06	48.52	0.06	13.33	0.02	48.91	0.02
MiniGPT4	52.27	0.03	55.41	0.04	52.03	0.05	55.41	0.04	**36.02**	0.03	46.88	0.01
mPLUG-Owl	59.98	0.02	88.66	0.02	51.86	0.03	75.08	0.02	20.09	0.05	46.53	0.00
PandaGPT	48.78	0.06	76.86	0.06	43.89	0.08	24.21	0.11	27.03	0.11	48.02	0.00
IB-LLM	48.66	0.03	83.8	0.02	43.18	0.05	48.31	0.04	14.63	0.03	46.53	0.00
LA-V2	30.83	0.09	62.14	0.08	24.49	0.00	47.27	0.08	12.96	0.04	46.53	0.00
mmGPT	41.78	0.04	93.34	0.04	45.02	0.08	41.53	0.06	13.70	0.05	46.53	0.00
Shikra	50.86	0.01	89.70	0.02	47.99	0.10	53.77	0.04	28.70	0.03	**57.48**	0.04
Lynx	**67.73**	0.03	87.86	0.03	56.47	0.07	**75.85**	0.04	20.09	0.07	47.23	0.01
$Cheetor_V$	49.36	0.05	87.30	0.03	47.88	0.09	43.06	0.11	22.22	0.10	50.30	0.05
$Cheetor_{L_2}$	45.35	0.07	**96.88**	0.02	38.13	0.09	39.07	0.10	18.89	0.06	46.58	0.02
BLIVA	59.36	0.04	94.78	0.01	**58.27**	0.04	67.10	0.04	19.35	0.03	48.02	0.03

Table 9: Evaluation results on coarse-grained perception. “Acc” and “Instby” are short for accuracy and instability, respectively.

performs well on these tasks while BLIP-2 and InstructBLIP perform relatively poorly. However, BLIP-2 and InstructBLIP are able to distinguish these categories if provided in the question, enabling them to perform well under generation evaluation.

C.1.2 Results on Fine-grained Perception

Tabel 11 and Table 12 provide results of fine-grained perception tasks, including Object Perception and Object Grounding. For object perception, BLIP-2 and InstructBLIP dominate most tasks, especially when evaluated with the generation evaluation strategy. Under likelihood evaluation, the effectiveness of BLIVA is demonstrated, indicating that incorporating patch features helps the model to perceive fine-grained information. Additionally, Lynx is a strong competitor in object-perception tasks benefiting from its enhanced visual representations. Considering the results of $MSCOCO_{goi}$, most models are able to solve a part of the questions, indicating that LVLMs are able to understand the bounding boxes in images and the grounded questions. Bounding box labeling can be an optional method to provide locality information without the need for understanding continuous input. As for object grounding, the task is quite difficult for most models. Only BLIP-2 and InstructBLIP perform well under generation evaluation, but they still struggle under likelihood evaluation. We speculate that this is because there are only subtle differences between options in these questions, such as “the person on the left” and “the person on the right”. In generation evaluation, all options are provided in the context, helping the models with strong instruct understanding abilities to distinguish between them. As for likelihood evaluation, options are provided to the model separately, models may not be able to distinguish them effectively.

Model	Scene Recognition						Avg.	
	$\text{TDIUC}_{\text{sport}}$		$\text{TDIUC}_{\text{scene}}$		$\text{MEDIC}_{\text{dts}}$			
	Acc	Instability	Acc	Instability	Acc	Instability	Acc	Instability
Generation Evaluation								
BLIP-2$_F$	93.75	0.12	88.66	0.04	60.29	0.25	69.44	0.10
InstructBLIP$_F$	**93.79**	0.12	**89.27**	0.05	**60.76**	0.15	**71.18**	0.07
InstructBLIP$_V$	90.62	0.20	69.78	0.09	52.00	0.13	69.06	0.12
LLaVA$_V$	39.29	1.17	28.47	1.00	34.67	0.48	28.69	0.66
LLaVA$_{L_2}$	74.13	0.51	67.29	0.16	36.00	0.28	48.31	0.23
MiniGPT4	65.41	0.68	58.04	0.40	36.19	0.44	46.19	0.40
mPLUG-Owl	59.54	0.85	58.79	0.64	26.67	0.81	41.95	0.56
PandaGPT	22.39	1.35	38.04	0.86	14.95	0.66	28.19	0.53
IB-LLM	24.59	1.33	45.70	0.59	19.43	0.77	29.23	0.44
LA-V2	42.94	1.11	48.69	0.54	20.76	0.79	33.18	0.48
mmGPT	28.81	1.29	45.23	0.64	15.25	0.87	30.37	0.58
Shikra	78.26	0.43	60.56	0.53	34.00	0.27	47.21	0.22
Lynx	85.69	0.29	69.07	0.15	47.52	0.26	59.49	0.21
Cheetor$_V$	76.33	0.47	59.63	0.35	42.38	0.49	52.00	0.29
Cheetor$_{L_2}$	53.58	0.92	68.6	0.15	29.71	0.29	46.50	0.27
BLIVA	65.87	0.68	56.73	0.41	30.95	0.41	41.72	0.31
Likelihood Evaluation								
BLIP-2$_F$	96.32	0.05	89.90	0.02	48.00	0.05	60.70	0.04
InstructBLIP$_F$	96.9	0.05	91.21	0.01	46.10	0.09	60.35	0.04
InstructBLIP$_V$	**97.2**	0.04	90.98	0.01	38.57	0.52	58.54	0.10
LLaVA$_V$	92.67	0.11	89.53	0.08	**57.62**	0.20	60.98	0.07
LLaVA$_{L_2}$	76.33	0.32	80.47	0.19	42.76	0.40	49.94	0.13
MiniGPT4	87.52	0.19	68.88	0.12	39.62	0.37	54.89	0.10
mPLUG-Owl	80.91	0.28	64.02	0.27	34.19	0.28	57.92	0.11
PandaGPT	41.28	0.88	55.98	0.35	14.76	0.67	42.31	0.26
IB-LLM	78.53	0.35	55.61	0.33	26.95	0.25	49.58	0.12
LA-V2	71.28	0.42	63.93	0.22	24.57	0.49	42.67	0.16
mmGPT	82.11	0.27	71.87	0.07	37.24	0.36	52.57	0.11
Shikra	92.11	0.12	85.14	0.06	42.19	0.39	60.88	0.09
Lynx	96.24	0.07	**96.63**	0.03	46.86	0.31	**66.11**	0.07
Cheetor$_V$	88.81	0.18	77.29	0.08	38.48	0.36	56.08	0.12
Cheetor$_{L_2}$	78.90	0.31	72.24	0.06	38.10	0.29	52.68	0.11
BLIVA	96.33	0.05	93.83	0.10	47.14	0.19	64.91	0.06

Table 10: Supplement of Table 9

C.1.3 RESULTS ON SCENE TEXT PERCEPTION

Table 13 and Table 14 provide results of scene text perception, which consists of OCR, Grounded OCR, KIE and OCR-based VQA tasks. Since the scene text perception task requires the model output to contain the target tokens in the image, only generation evaluation is conducted. InstructBLIP consistently dominates the OCR task, while mPLUG-Owl and BLIVA take the lead on GroundOCR, KIE and OCR-based VQA tasks. mPLUG-Owl also performs well on OCR task. OCR-related tasks depend heavily on the image comprehension capability of visual backbones, hence we attribute the stable performance of mPLUG-Owl to its special pre-training procedure, as it is the only LVLM that trains the visual backbone during pre-training. Similarly, BLIVA utilizes additional encoded patch embeddings to improve the understanding of text within images. Therefore, enhancing the understanding and utilization of visual content is key to promoting improvements in scene text perception.

C.1.4 RESULTS ON VISUALLY GROUNDED REASONING

Table 15 and Table 16 provide results of visually grounded reasoning, which consists of VQA and KVQA. For generation evaluation, BLIP-2$_\text{F}$ and InstructBLIP$_\text{F}$ achieve top-2 performance on nearly all the datasets for VGR tasks. While in likelihood evaluation, InstructBLIP$_\text{V}$, Lynx and BLIVA

Model	Object Perception									
	$\text{TDIUC}_{\text{color}}$		$\text{TDIUC}_{\text{utility}}$		$\text{TDIUC}_{\text{position}}$		$\text{TDIUC}_{\text{detection}}$		$\text{TDIUC}_{\text{counting}}$	
	Acc	Instability	Acc	Instability	Acc	Instability	Acc	Instability	Acc	Instability
Generation Evaluation										
BLIP-2$_F$	73.90	0.45	92.40	0.09	**91.55**	0.19	**99.38**	0.02	71.00	0.54
InstructBLIP$_F$	**78.22**	0.39	**95.56**	0.03	90.26	0.22	98.77	0.03	**73.05**	0.50
InstructBLIP$_V$	69.19	0.58	89.01	0.09	81.29	0.42	97.26	0.07	61.76	0.77
LLaVA$_V$	8.25	1.46	57.89	0.80	30.60	1.33	53.29	0.97	23.43	1.43
LLaVA$_{L_2}$	57.02	0.83	85.85	0.20	68.70	0.69	91.78	0.20	43.14	1.10
MiniGPT4	46.48	1.03	72.16	0.51	56.21	0.95	83.77	0.39	42.38	1.12
mPLUG-Owl	28.20	1.32	55.67	0.83	40.86	1.23	60.41	0.89	28.10	1.32
PandaGPT	30.18	1.27	57.19	0.79	27.59	1.38	61.99	0.85	26.52	1.33
IB-LLM	25.17	1.36	42.69	1.04	31.12	1.37	39.93	1.26	28.10	1.33
LA-V2	26.48	1.33	40.58	1.08	29.66	1.40	43.90	1.19	25.10	1.35
mmGPT	27.10	1.32	38.71	1.11	26.29	1.43	38.63	1.27	25.33	1.35
Shikra	39.43	1.15	61.64	0.69	50.43	1.00	61.23	0.85	27.67	0.43
Lynx	68.93	0.61	84.91	0.19	64.31	0.76	91.85	0.2	33.95	1.22
Cheetor$_V$	47.10	1.01	78.01	0.34	49.91	1.05	85.34	0.34	35.71	1.22
Cheetor$_{L_2}$	54.57	0.84	81.52	0.29	57.76	0.90	84.72	0.37	31.29	1.26
BLIVA	44.28	1.06	61.75	0.68	45.09	1.14	63.49	0.82	41.95	1.13
Likelihood Evaluation										
BLIP-2$_F$	79.83	0.34	91.35	0.10	94.66	0.12	98.84	0.03	82.43	0.31
InstructBLIP$_F$	90.46	0.16	**93.80**	0.07	94.91	0.11	**99.45**	0.01	**82.95**	0.29
InstructBLIP$_V$	**91.64**	0.15	91.35	0.14	**95.78**	0.10	99.11	0.02	79.86	0.33
LLaVA$_V$	70.44	0.48	83.27	0.12	77.59	0.46	97.05	0.06	62.23	0.59
LLaVA$_{L_2}$	55.72	0.72	82.81	0.21	71.90	0.59	91.10	0.20	74.71	0.44
MiniGPT4	69.92	0.49	86.90	0.13	76.12	0.49	96.37	0.09	73.19	0.46
mPLUG-Owl	57.75	0.68	90.41	0.10	75.69	0.52	93.22	0.15	71.00	0.49
PandaGPT	45.07	0.87	67.95	0.45	47.59	1.02	76.16	0.51	45.19	0.97
IB-LLM	36.14	0.92	82.22	0.25	63.53	0.73	81.16	0.39	23.95	1.09
LA-V2	55.72	0.72	88.70	0.15	69.57	0.64	83.84	0.35	54.33	0.7
mmGPT	44.96	0.85	86.32	0.14	74.74	0.54	95.82	0.10	63.81	0.62
Shikra	58.07	0.67	86.67	0.16	73.10	0.55	88.22	0.25	74.24	0.43
Lynx	82.61	0.31	87.37	0.15	92.84	0.16	98.36	0.04	81.33	0.34
Cheetor$_V$	72.74	0.46	82.69	0.16	80.60	0.42	98.08	0.05	70.90	0.49
Cheetor$_{L_2}$	61.15	0.64	66.32	0.55	75.43	0.50	92.05	0.18	50.48	0.76
BLIVA	89.87	0.18	92.05	0.07	95.17	0.11	99.25	0.02	82.57	0.29

Table 11: Evaluation results on fine-grained perception.

also exhibit some outstanding performance. As discussed in Section 4.3.4, likelihood evaluation performances of many models are significantly better than generation.

We also conducted a hierarchical evaluation of LVLMs' external knowledge incorporation and reasoning abilities. Comparing the results of ViQuAE and K-ViQuAE, as well as A-OKVQA and A-OKVQRA, it is evident that, with the provision of external knowledge, the performance of most models has significantly improved.

In addition, it can be observed that, except for models based on FlanT5 and LLaMA2-Chat, the generation performance of other models on the A-OKVQAR dataset is significantly lower than the likelihood performance. This may be attributed to the fact that the rationale options are often longer, and for language models with weaker instruction-following capabilities (as mentioned in Section 4.3.4), memory lapses may occur during generation, thereby affecting performance.

C.1.5 Results on Spatial Understanding

Table 17 provides results of the spatial understanding capability dimension, which includes relation judgment and space-based perception tasks. For generation evaluation, BLIP-2 and InstructBLIP dominate in most tasks. For likelihood evaluation, although BLIP-2 and InstructBLIP still perform well, Lynx and BLIVA start to hold leadership positions. We attribute this to the fact that BLIP-2, InstructBLIP, Lynx and BLIVA uses relatively high-quality MSCOCO data. As the images in VSR dataset are retrieved from COCO 2017, models tend to have better performance on this dataset.

For the spatial relation judgment task, the performance on the MP3D-Spatial dataset is relatively poor. We believe the reason for this is that MP3D-Spatial is sampled from real navigation environments, which are inherently more complex. For space-based perception tasks, likelihood evalua-

Model	Object Perception								Object Grounding		Avg.	
	MSCOCO$_{count}$		**MSCOCO$_{mci}$**		**MSCOCO$_{goi}$**		**MSCOCO$_{mos}$**		**RefCOCO$_{res}$**			
	Acc	Instability	Acc	Instability	Acc	Instability	Acc	Instability	Acc	Instability	Acc	Instability
Generation Evaluation												
BLIP-2$_F$	**87.48**	0.26	82.22	0.09	59.50	0.09	39.11	0.21	69.58	0.20	76.61	0.21
InstructBLIP$_F$	87.25	0.26	**84.72**	0.08	63.05	0.11	37.65	0.28	**72.75**	0.12	**78.13**	0.20
InstructBLIP$_V$	64.02	0.76	83.17	0.17	**64.94**	0.24	39.27	0.55	57.58	0.24	70.75	0.39
LLaVA$_V$	18.60	1.48	44.88	0.91	29.56	1.14	34.66	0.94	42.41	0.38	34.36	1.08
LLaVA$_{L_2}$	40.78	1.16	64.67	0.48	53.33	0.36	41.54	0.64	50.75	0.30	59.76	0.60
MiniGPT4	35.95	1.24	58.50	0.66	53.06	0.61	41.94	0.68	41.00	0.29	53.15	0.75
mPLUG-Owl	28.07	1.33	31.00	1.02	30.94	1.04	36.60	0.91	32.08	0.78	37.19	1.07
PandaGPT	22.92	1.40	25.11	1.03	25.16	1.01	41.54	0.70	28.08	0.47	34.63	1.02
IB-LLM	28.54	1.32	32.06	0.90	30.67	0.85	40.24	0.89	28.75	0.62	32.73	1.09
LA-V2	26.43	1.34	22.33	1.06	21.11	1.11	42.02	0.72	30.75	0.76	30.84	1.13
mmGPT	22.34	1.40	30.33	1.00	27.56	1.01	41.38	0.75	25.58	0.93	30.33	1.16
Shikra	29.04	1.31	70.50	0.44	54.61	0.57	28.91	0.57	51.75	0.22	47.52	0.72
Lynx	51.07	1.00	73.56	0.37	60.78	0.30	**42.19**	0.42	54.67	0.40	62.62	0.55
Cheetor$_V$	29.63	1.29	49.67	0.78	45.11	0.72	38.78	0.70	43.75	0.52	50.30	0.80
Cheetor$_{L_2}$	30.57	1.29	52.16	0.66	43.16	0.66	40.32	0.67	37.42	0.46	51.35	0.74
BLIVA	37.93	1.20	39.94	0.82	32.22	0.89	40.00	0.67	27.58	0.35	43.42	0.88
Likelihood Evaluation												
BLIP-2$_F$	77.31	0.41	81.77	0.02	60.39	0.02	39.27	0.02	38.58	0.15	74.44	0.15
InstructBLIP$_F$	73.14	0.48	82.94	0.04	60.44	0.05	42.27	0.06	36.08	0.09	75.64	0.14
InstructBLIP$_V$	89.98	0.17	**84.72**	0.02	64.94	0.02	**43.89**	0.04	37.17	0.11	77.84	0.11
LLaVA$_V$	91.07	0.16	76.22	0.12	62.50	0.15	39.92	0.15	43.00	0.15	70.33	0.24
LLaVA$_{L_2}$	89.01	0.20	64.44	0.17	47.44	0.12	40.24	0.13	38.33	0.09	65.57	0.29
MiniGPT4	87.56	0.22	77.11	0.06	58.22	0.06	41.62	0.07	38.50	0.10	70.55	0.22
mPLUG-Owl	89.04	0.20	56.61	0.13	49.56	0.14	38.38	0.10	39.33	0.10	66.10	0.26
PandaGPT	66.04	0.60	32.22	0.29	26.94	0.31	42.11	0.28	24.50	0.13	47.38	0.54
IB-LLM	87.06	0.22	48.61	0.09	41.78	0.13	43.72	0.09	35.92	0.10	54.41	0.40
LA-V2	87.45	0.22	49.83	0.08	46.83	0.16	41.21	0.09	36.67	0.11	61.42	0.32
mmGPT	69.12	0.56	61.56	0.11	52.19	0.37	43.08	0.10	32.33	0.08	62.39	0.35
Shikra	90.21	0.17	51.56	0.10	54.67	0.10	41.70	0.08	**49.92**	0.11	66.84	0.26
Lynx	88.97	0.18	80.22	0.08	65.28	0.09	42.02	0.12	43.42	0.09	76.24	0.16
Cheetor$_V$	77.66	0.40	74.67	0.08	55.67	0.12	43.07	0.14	33.42	0.16	68.95	0.25
Cheetor$_{L_2}$	80.16	0.36	67.88	0.09	51.56	0.11	39.92	0.12	32.00	0.13	61.70	0.34
BLIVA	**94.04**	0.10	84.00	0.03	**66.72**	0.04	42.35	0.06	35.75	0.13	**78.18**	0.10

Table 12: Supplement of Table 11

Model	OCR						Grounded OCR		
	CUTE80	**IC15**	**IIIT5K**	**COCO-Text**	**WordArt**	**TextOCR**	**gIC15**	**gCOCO-Text**	**gTextOCR**
Generation Evaluation									
BLIP-2$_F$	80.07	64.75	72.27	50.54	72.32	68.40	61.43	16.27	32.60
InstructBLIP$_F$	**84.17**	**75.36**	**83.40**	**56.66**	**75.76**	**74.27**	55.24	17.33	32.60
InstructBLIP$_V$	81.60	73.15	77.20	53.00	74.17	70.60	53.33	18.93	32.13
LLaVA$_V$	26.11	23.65	25.73	13.00	34.44	36.00	40.24	17.33	30.00
LLaVA$_{L_2}$	32.15	25.75	27.20	15.83	40.13	39.87	43.57	17.93	32.07
MiniGPT4	71.39	58.90	71.67	40.36	72.45	60.27	44.05	11.00	28.60
mPLUG-Owl	73.68	60.77	74.67	46.39	73.25	64.27	64.52	20.27	34.67
PandaGPT	1.60	1.88	3.13	0.14	5.03	26.87	0.24	0.40	22.73
IB-LLM	11.94	8.95	8.60	2.41	11.66	29.73	6.19	3.33	23.80
LA-V2	36.53	31.82	35.33	17.82	40.13	42.13	47.86	18.07	33.20
mmGPT	26.94	23.09	18.80	13.43	31.13	36.20	26.43	12.73	28.80
Shikra	2.57	4.75	5.07	4.33	9.54	31.13	29.76	5.93	27.53
Lynx	34.03	25.08	20.93	11.51	37.22	36.00	32.86	10.60	30.80
Cheetor$_V$	52.50	39.01	53.87	29.73	56.16	52.27	40.00	11.20	28.20
Cheetor$_{L_2}$	42.78	31.38	39.20	20.36	34.83	45.40	16.67	6.67	25.13
BLIVA	77.29	68.40	72.47	51.49	71.26	66.93	**64.76**	**21.67**	**37.27**

Table 13: Evaluation results on scene text perception.

tion yields better results than generation evaluation, especially for LLaVA, mPLUG-Owl, LA-V2, mmGPT, Shikra and Cheetor. This might be attributed to the high demand for spatial reasoning skills for this task, thereby placing a greater emphasis on the image comprehension abilities of visual backbones. Most of these models use ViT-L, which lacks robust spatial semantic understanding.

C.1.6 Results on Cross-modal Inference

Table 18 provides results of the cross-modal inference capability dimension, which includes image-text matching tasks and visual entailment tasks. For the image-text matching task in MSCOCO, we consider a one-to-one setup of the naive image-text matching and a one-to-four selection setup of image-text selection. BLIP-2 and Instruct BLIP perform well in both setups under the generation

Model	KIE			OCR-based VQA			Avg.
	SROIE	POIE	FUNSD	TextVQA	DocVQA	OCR-VQA	
Generation Evaluation							
BLIP-2$_F$	1.30	0.76	1.72	21.47	5.39	21.62	38.06
InstructBLIP$_F$	0.87	0.44	2.07	26.76	4.78	28.07	**41.19**
InstructBLIP$_V$	3.48	0.82	1.72	30.22	6.21	34.37	40.73
LLaVA$_V$	0.00	0.44	1.72	19.02	3.13	5.74	18.44
LLaVA$_{L_2}$	0.00	1.21	1.72	26.31	6.52	12.13	21.49
MiniGPT4	0.29	0.85	2.07	17.29	3.95	12.49	33.04
mPLUG-Owl	**4.06**	1.58	1.72	**30.71**	**8.40**	**37.87**	39.79
PandaGPT	0.00	0.09	1.72	0.80	2.22	0.00	4.46
IB-LLM	0.00	0.06	1.72	10.09	3.62	0.91	8.20
LA-V2	0.72	**3.16**	1.72	30.40	8.06	16.40	24.22
mmGPT	0.00	1.33	1.72	21.07	4.78	4.47	16.73
Shikra	0.00	0.82	1.72	1.56	0.19	0.25	8.34
Lynx	0.00	1.58	1.72	24.71	4.11	7.61	18.58
Cheetor$_V$	0.14	0.79	1.72	13.16	3.62	7.26	25.90
Cheetor$_{L_2}$	0.00	0.57	1.72	11.02	4.11	3.05	18.83
BLIVA	2.61	3.04	**3.45**	29.69	6.18	34.97	40.77

Table 14: Supplement of Table 13.

Model	VQA						KVQA					
	GQA		VQA v2		Whoops		OK-VQA		ScienceQA		VizWiz	
	Acc	Instability	Acc	Instability	Acc	Instability	Acc	Instability	Acc	Instability	Acc	Instability
Generation Evaluation												
BLIP-2$_F$	62.66	0.18	69.86	0.19	**81.96**	0.10	68.97	0.23	**63.78**	0.27	**82.13**	0.12
InstructBLIP$_F$	**66.11**	0.19	**74.31**	0.16	80.04	0.08	**70.87**	0.15	62.19	0.26	74.90	0.18
InstructBLIP$_V$	59.09	0.31	62.59	0.32	71.96	0.27	63.73	0.36	58.01	0.42	49.37	0.41
LLaVA$_V$	37.26	0.80	46.01	0.55	50.48	0.69	41.59	0.78	46.57	0.63	31.37	0.80
LLaVA$_{L_2}$	52.36	0.43	51.65	0.40	57.14	0.43	54.09	0.57	57.91	0.49	40.32	0.54
MiniGPT4	44.57	0.66	46.49	0.64	47.08	0.78	38.65	0.88	43.78	0.71	35.22	0.83
mPLUG-Owl	34.56	0.89	35.48	0.88	37.44	0.93	33.45	0.97	41.39	0.80	30.63	0.96
PandaGPT	38.07	0.67	37.28	0.68	24.64	0.85	29.80	0.90	44.48	0.69	24.87	0.89
IB-LLM	38.63	0.75	38.56	0.77	27.86	0.95	31.67	0.96	41.49	0.73	26.22	0.97
LA-V2	40.21	0.68	39.27	0.67	34.17	0.94	29.52	1.00	41.59	0.76	28.63	0.93
mmGPT	35.12	0.85	34.47	0.85	27.20	1.01	27.34	1.00	40.10	0.78	23.67	0.95
Shikra	41.69	0.73	44.93	0.67	50.48	0.73	41.15	0.86	38.61	0.72	41.81	0.81
Lynx	55.88	0.47	60.14	0.43	67.02	0.41	55.75	0.55	53.63	0.49	49.65	0.61
Cheetor$_V$	46.17	0.58	48.17	0.56	55.71	0.64	43.49	0.78	47.06	0.63	37.59	0.78
Cheetor$_{L_2}$	48.39	0.42	45.62	0.43	42.26	0.51	44.64	0.61	56.12	0.50	32.76	0.65
BLIVA	43.40	0.58	50.06	0.01	46.31	0.76	36.75	0.76	42.09	0.65	35.64	0.80
Likelihood Evaluation												
BLIP-2$_F$	62.70	0.06	69.37	0.06	70.95	0.04	66.83	0.07	53.93	0.03	76.71	0.08
InstructBLIP$_F$	66.65	0.06	79.67	0.05	68.99	0.04	76.35	0.03	56.32	0.03	62.92	0.04
InstructBLIP$_V$	**67.76**	0.04	**82.92**	0.02	72.32	0.02	**82.82**	0.02	57.91	0.02	57.17	0.03
LLaVA$_V$	54.14	0.12	58.94	0.09	65.36	0.06	62.18	0.11	54.03	0.08	40.28	0.07
LLaVA$_{L_2}$	52.68	0.09	51.81	0.10	60.06	0.06	48.77	0.15	55.22	0.09	47.05	0.09
MiniGPT4	56.10	0.06	56.04	0.06	63.15	0.05	55.08	0.10	51.74	0.04	49.00	0.05
mPLUG-Owl	50.95	0.06	50.53	0.07	60.89	0.05	49.80	0.10	50.25	0.04	44.32	0.09
PandaGPT	41.35	0.20	37.86	0.25	28.69	0.20	36.11	0.24	43.88	0.13	19.12	0.17
IB-LLM	46.86	0.03	47.06	0.03	48.93	0.04	45.52	0.05	54.03	0.03	32.71	0.05
LA-V2	50.29	0.06	47.36	0.05	60.71	0.06	44.60	0.10	50.05	0.03	41.21	0.08
mmGPT	52.86	0.06	48.54	0.06	49.64	0.06	56.43	0.10	49.25	0.03	38.93	0.06
Shikra	57.07	0.09	64.38	0.07	65.83	0.06	59.72	0.08	51.54	0.06	42.00	0.04
Lynx	69.21	0.12	73.82	0.10	**73.21**	0.05	68.97	0.11	55.52	0.05	**79.44**	0.04
Cheetor$_V$	58.71	0.09	59.70	0.09	62.86	0.08	58.81	0.11	48.26	0.08	44.73	0.13
Cheetor$_{L_2}$	53.03	0.08	50.13	0.10	56.55	0.09	50.63	0.13	55.42	0.06	35.96	0.11
BLIVA	67.37	0.05	81.36	0.03	69.88	0.03	78.53	0.03	**60.70**	0.02	51.32	0.04

Table 15: Evaluation results on visually grounded reasoning.

evaluation. However, the performance is not satisfactory under the likelihood evaluation for image-text selection, we attribute this to the same reason that is mentioned in the analysis of referring expression selection in Appendix C.1.2. Unlike MSCOCO, WikiHow considers the scenarios to match images and abstract instructions, while Winogroud uses negative options with only minor word-level modifications. These pose significant challenges for the models, resulting in a noticeable decrease in accuracy. However, InstructBLIP maintains a lead. Regarding the visual entailment task, apart from the two models based on FlanT5, the performance of the other models is not promising. In summary, we believe that current LVLMs still have relatively weak capabilities in logical reasoning and understanding fine-grained textual details.

Model	KVQA												Avg.	
	ViQuAE		K-ViQuAE		A-OKVQA		A-OKVQRA		A-OKVQAR		ImageNetVC			
	Acc	Instability	Acc	Instability	Acc	Instability	Acc	Instability	Acc	Instability	Acc	Instability	Acc	Instability
Generation Evaluation														
BLIP-2$_F$	44.32	0.37	**87.26**	0.10	71.40	0.18	85.61	0.07	80.00	0.17	**81.72**	0.14	73.31	0.18
InstructBLIP$_F$	43.68	0.36	87.10	0.09	**77.02**	0.17	**89.82**	0.05	**81.23**	0.16	79.07	0.14	**73.86**	0.17
InstructBLIP$_V$	**49.76**	0.41	80.32	0.26	71.58	0.28	79.47	0.24	47.72	0.61	62.56	0.30	63.01	0.35
LLaVA$_V$	39.52	0.77	50.00	0.73	42.56	0.78	62.11	0.62	31.58	0.83	48.94	0.49	44.00	0.71
LLaVA$_{L_2}$	47.20	0.50	85.00	0.17	60.18	0.47	81.93	0.24	61.93	0.40	66.58	0.30	59.69	0.41
MiniGPT4	32.48	0.91	65.81	0.56	39.65	0.85	59.30	0.67	40.18	0.82	53.81	0.57	45.59	0.74
mPLUG-Owl	31.04	0.99	51.29	0.81	35.26	1.01	41.58	0.88	35.61	0.90	42.65	0.79	37.53	0.90
PandaGPT	39.84	0.74	74.68	0.37	29.82	0.94	63.16	0.62	39.82	0.76	56.81	0.55	41.94	0.72
IB-LLM	29.28	0.97	46.13	0.86	29.65	0.96	54.56	0.76	32.28	1.01	44.32	0.70	36.72	0.87
LA-V2	27.20	1.00	40.32	0.90	31.75	0.99	47.02	0.86	31.93	0.90	43.78	0.56	36.28	0.85
mmGPT	31.04	0.99	45.81	0.90	24.39	1.00	38.42	0.93	25.26	0.95	43.14	0.73	33.00	0.91
Shikra	29.92	0.95	38.71	0.86	41.93	0.83	40.53	0.86	37.19	0.78	47.13	0.65	41.17	0.79
Lynx	39.68	0.65	72.42	0.41	65.09	0.46	79.30	0.28	37.54	0.85	64.08	0.37	58.35	0.50
Cheetor$_V$	40.48	0.80	70.00	0.48	41.05	0.76	63.33	0.59	48.42	0.68	56.81	0.51	49.86	0.65
Cheetor$_{L_2}$	44.16	0.57	82.26	0.22	48.42	0.54	82.28	0.22	57.37	0.50	68.50	0.26	54.40	0.45
BLIVA	33.92	0.76	45.16	0.85	44.21	0.71	54.74	0.74	31.05	0.77	45.70	0.56	42.42	0.66
Likelihood Evaluation														
BLIP-2$_F$	38.72	0.10	87.26	0.01	64.74	0.08	81.58	0.03	**84.04**	0.01	80.34	0.07	69.76	0.05
InstructBLIP$_F$	33.12	0.05	**88.71**	0.02	70.88	0.06	79.82	0.03	83.86	0.01	84.47	0.05	70.98	0.04
InstructBLIP$_V$	46.88	0.05	82.26	0.01	78.25	0.01	86.67	0.04	81.40	0.03	**85.70**	0.02	**73.51**	0.03
LLaVA$_V$	39.20	0.10	75.00	0.07	59.30	0.09	73.51	0.12	61.40	0.05	63.34	0.07	58.89	0.09
LLaVA$_{L_2}$	35.36	0.17	80.48	0.06	48.25	0.14	64.74	0.09	68.95	0.01	67.17	0.10	56.71	0.10
MiniGPT4	27.68	0.08	73.23	0.03	57.72	0.07	70.35	0.06	64.21	0.03	62.80	0.05	57.26	0.06
mPLUG-Owl	30.24	0.09	78.87	0.08	42.98	0.10	63.51	0.09	67.89	0.02	61.03	0.06	54.27	0.07
PandaGPT	24.64	0.26	77.26	0.07	31.75	0.25	59.30	0.14	61.93	0.05	57.44	0.17	43.28	0.18
IB-LLM	32.80	0.05	67.42	0.08	44.39	0.04	58.42	0.10	66.32	0.04	58.92	0.02	50.28	0.05
LA-V2	39.20	0.05	70.00	0.08	43.51	0.07	70.88	0.07	66.49	0.03	64.28	0.05	54.05	0.06
mmGPT	33.44	0.10	82.58	0.07	49.47	0.09	69.47	0.10	77.54	0.01	66.19	0.05	56.20	0.07
Shikra	35.20	0.10	65.65	0.04	57.72	0.07	64.74	0.11	75.26	0.00	62.56	0.09	58.47	0.07
Lynx	41.92	0.15	80.32	0.05	64.56	0.10	77.02	0.16	78.42	0.01	76.86	0.12	69.94	0.09
Cheetor$_V$	34.40	0.10	70.81	0.07	59.12	0.11	70.88	0.09	70.18	0.02	66.29	0.06	58.73	0.09
Cheetor$_{L_2}$	37.12	0.13	82.26	0.06	53.33	0.10	73.51	0.08	74.91	0.02	66.78	0.11	57.47	0.09
BLIVA	**51.84**	0.06	83.87	0.02	**80.53**	0.03	**87.72**	0.01	79.12	0.02	82.95	0.04	72.93	0.03

Table 16: Supplement of Table 15.

C.1.7 RESULTS ON VISUAL DESCRIPTION

Table 19 provides image captioning results of the visual description capability dimension. As mentioned in previous work (Xu et al., 2023), these datasets require concise captions while most LVLMs tend to generate detailed descriptions. Therefore, the performance of most models is not satisfying enough. For this task, PandaGPT always generates a sentence starting with “the image features” and the performance is limited. At the same time, BLIP-2 dominates the task because BLIP-2 is able to provide short captions. To adapt to the development of LVLMs, there is a strong need for a benchmark for evaluating detailed description capabilities.

C.1.8 RESULTS ON MULTI-TURN DIALOGUE

Table 20 provides results of the multi-turn Dialogue task. BLIP-2 and InstructBLIP perform the best in this task while BLIVA takes second place under likelihood evaluation. For VQA-MT, there is no inter-turn dependency, and there is no obvious common relationship between the performance and the number of dialogue turns. However, for VisDial where strong dependencies exist between the proceeding and following questions, LVLMs generally perform worse in multi-turn dialogues where models face more complex contexts. Moreover, the performance of LVLMs deteriorates with the increase in dialogue turns. We hypothesize the reason is that single-turn image-text pairs dominate the training data of LVLMs. Multi-turn data should be incorporated during training to further improve existing LVLMs. Additionally, the advantages of some models like BLIVA and Shikra are only demonstrated with the likelihood evaluation method, this phenomenon has been discussed in Section 4.3.4

C.2 EFFECT OF IN-CONTEXT SAMPLE

Table 21 provides the complete results for Section 4.3.3. The models that are not previously mentioned already possess strong abilities to follow single-choice instructions, either through the introduction of language-only instruction-following data during training (ImageBind-LLM) or through the inherent abilities of the frozen backbones like Vicuna (Chiang et al., 2023), LLaMA2-Chat (Touvron et al., 2023b), and OpenFlamingo. These models are able to generate option marks for most questions, however, the in-context samples still assist in addressing issues on the remaining samples. For qualitative analysis, we provide some examples in Figure 11, the questions are from VQA v2.

Model	Space-based Perception		Spatial Relation Judgment				Avg.	
	CLEVR		VSR		MP3D-Spatial			
	Acc	Instability	Acc	Instability	Acc	Instability	Acc	Instability
Generation Evaluation								
BLIP-2_F	42.67	0.28	46.95	0.21	<u>39.87</u>	0.32	43.16	0.27
InstructBLIP$_F$	<u>44.84</u>	0.39	<u>52.37</u>	0.25	**41.01**	0.37	**46.07**	0.34
InstructBLIP$_V$	**46.32**	0.51	<u>52.37</u>	0.49	34.59	0.50	<u>44.43</u>	0.50
LLaVA$_V$	19.01	1.24	40.00	0.88	27.19	1.13	28.73	1.08
LLaVA$_{L_2}$	36.52	0.61	**52.54**	0.21	34.67	0.64	41.24	0.49
MiniGPT4	33.74	0.84	36.44	0.81	33.62	0.84	34.60	0.83
mPLUG-Owl	27.48	1.01	28.81	0.97	24.23	1.04	26.84	1.01
PandaGPT	29.65	0.90	35.76	0.86	34.50	0.80	33.30	0.85
IB-LLM	31.45	0.96	40.00	0.94	35.22	0.83	35.56	0.91
LA-V2	21.39	1.05	23.05	1.04	27.06	1.01	23.83	1.03
mmGPT	22.26	1.13	28.98	1.01	29.30	0.98	26.85	1.04
Shikra	23.82	0.77	46.27	0.60	29.77	0.84	33.29	0.74
Lynx	40.58	0.68	45.76	0.66	34.38	0.78	40.24	0.71
Cheetor$_V$	24.72	1.03	35.76	0.77	31.21	0.88	30.56	0.89
Cheetor$_{L_2}$	29.10	0.77	40.85	0.69	33.53	0.73	34.49	0.73
BLIVA	30.64	0.85	35.25	0.61	34.12	0.59	33.34	0.68
Likelihood Evaluation								
BLIP-2_F	48.78	0.05	61.36	0.11	43.21	0.13	51.12	0.10
InstructBLIP$_F$	48.29	0.08	60.51	0.17	<u>44.82</u>	0.12	51.21	0.12
InstructBLIP$_V$	**53.19**	0.06	59.15	0.19	44.40	0.16	<u>52.25</u>	0.14
LLaVA$_V$	38.96	0.24	52.54	0.21	35.81	0.31	42.44	0.25
LLaVA$_{L_2}$	45.73	0.22	59.66	0.16	36.66	0.22	47.35	0.20
MiniGPT4	49.37	0.39	57.12	0.17	41.18	0.21	49.22	0.26
mPLUG-Owl	46.14	0.18	59.15	0.17	40.59	0.22	48.63	0.19
PandaGPT	36.67	0.31	52.03	0.29	29.60	0.33	39.43	0.31
IB-LLM	43.39	0.20	54.07	0.16	40.89	0.20	46.12	0.19
LA-V2	42.92	0.14	60.85	0.15	42.16	0.18	48.64	0.16
mmGPT	49.91	0.15	50.85	0.23	40.85	0.20	47.20	0.19
Shikra	42.72	0.11	57.12	0.25	36.62	0.23	45.49	0.20
Lynx	<u>51.77</u>	0.12	**66.27**	0.13	43.63	0.25	**53.89**	0.17
Cheetor$_V$	48.61	0.20	60.00	0.19	36.49	0.33	48.37	0.24
Cheetor$_{L_2}$	47.33	0.20	58.31	0.18	40.34	0.20	48.66	0.19
BLIVA	46.52	0.05	<u>63.39</u>	0.20	**45.20**	0.18	51.70	0.14

Table 17: Evaluation results on spatial understanding.

C.3 Effect of Model Parameters

We also examine the effect of model parameters on different evaluations, and these model parameters are categorized into four types, including number of total parameters (#oP), number of trainable parameters (#oTP), number of trainable LLM parameters (#oLTP), and number of visual tokens (#oVT). According to evaluation results, we consider the score of each model in a single task as an individual sample. These samples are partitioned into multiple groups based on different parameter scales and we generate boxplots for each group, shown in Figure 8 and Figure 9.

For the impact of total parameters on evaluation results, we round the parameters into three groups, including "4B", "7B", and "8B". BLIP-2 and InstructBLIP achieve superior results with fewer parameters, utilizing FlanT5-XL LLM. Except that, in the range from 7B to 8B, the score exhibits an increasing tendency with growth in total parameters.

For the effect of trainable parameters, it is observed that trainable parameters range of 100M to 1B may be an ideal scenario. Further, by analyzing different scales of trainable parameters from 0 to 1B, we conclude that: (1) For models with trainable parameters scales of 0-10M, primarily linear layers are trained but still achieve competitive results on these evaluation tasks. (2) For models with 10-100M trainable parameters, all of them implement LoRA or bias-tuning, and these parameter-efficient fine-tuning approaches even have negative impacts on generation and likelihood tasks. (3)

Model	ITM								VE				Avg.	
	MSCOCO$_{\text{itm}}$		**MSCOCO$_{\text{its}}$**		**WikiHow**		**Winoground**		**SNLI-VE**		**MOCHEG**			
	Acc	Instability	Acc	Instability	Acc	Instability	Acc	Instability	Acc	Instability	Acc	Instability	Acc	Instability
Generation Evaluation														
BLIP-2$_F$	96.40	0.04	97.53	0.02	33.67	0.26	55.25	0.32	72.20	0.15	**46.33**	0.02	66.90	0.14
InstructBLIP$_F$	**97.63**	0.02	**98.27**	0.01	**46.87**	0.20	**64.50**	0.25	**74.80**	0.11	46.09	0.24	**71.36**	0.14
InstructBLIP$_V$	63.73	0.24	96.33	0.04	33.13	0.17	55.00	0.51	32.33	0.00	42.07	0.19	53.76	0.19
LLaVA$_V$	51.40	0.10	77.67	0.23	29.47	0.47	46.00	0.55	35.87	0.33	43.37	0.31	47.30	0.33
LLaVA$_{L_2}$	52.17	0.01	87.20	0.11	34.00	0.29	49.00	0.42	33.13	0.07	44.02	0.56	49.91	0.24
MiniGPT4	52.20	0.00	61.87	0.26	27.87	0.36	53.00	0.57	37.33	0.29	40.36	0.65	45.44	0.36
mPLUG-Owl	51.63	0.19	42.00	0.68	26.20	0.79	49.50	0.56	36.60	0.62	36.33	0.65	40.38	0.58
PandaGPT	52.10	0.00	22.47	0.36	23.47	0.32	51.50	0.57	34.40	0.06	38.46	0.64	37.06	0.33
IB-LLM	51.87	0.13	29.20	0.43	21.53	0.54	48.75	0.54	32.07	0.54	35.92	0.66	36.56	0.47
LA-V2	52.20	0.00	42.00	0.73	25.93	0.83	48.00	0.54	37.00	0.69	41.24	0.14	41.06	0.49
mmGPT	51.73	0.29	32.00	0.87	24.47	0.86	50.25	0.59	32.33	0.59	38.34	0.57	38.19	0.63
Shikra	30.20	0.13	81.40	0.26	37.07	0.23	51.75	0.58	34.47	0.20	32.35	0.73	44.54	0.36
Lynx	51.13	0.08	91.33	0.12	33.27	0.43	55.25	0.51	50.07	0.41	36.92	0.67	53.00	0.37
Cheetor$_V$	53.60	0.08	71.47	0.33	31.40	0.62	53.00	0.52	35.13	0.49	39.88	0.63	47.41	0.45
Cheetor$_{L_2}$	52.27	0.02	52.67	0.32	30.40	0.31	50.50	0.49	32.80	0.01	45.44	0.50	44.01	0.28
BLIVA	50.50	0.55	67.27	0.29	30.47	0.33	47.00	0.58	33.80	0.22	42.25	0.47	45.22	0.41
Likelihood Evaluation														
BLIP-2$_F$	**96.37**	0.04	62.07	0.14	32.47	0.06	58.50	0.04	**57.73**	0.08	**46.33**	0.09	58.91	0.08
InstructBLIP$_F$	90.97	0.10	50.00	0.09	30.80	0.10	62.75	0.08	54.57	0.12	43.91	0.23	55.50	0.12
InstructBLIP$_V$	87.37	0.19	61.33	0.10	29.67	0.13	**68.00**	0.04	49.73	0.39	36.27	0.13	55.40	0.16
LLaVA$_V$	48.30	0.01	72.40	0.09	30.47	0.17	63.75	0.06	39.13	0.39	33.96	0.16	48.00	0.15
LLaVA$_{L_2}$	64.13	0.17	66.67	0.07	31.60	0.13	58.00	0.03	37.60	0.07	39.88	0.21	49.65	0.11
MiniGPT4	78.27	0.18	60.13	0.10	30.27	0.11	65.00	0.01	40.73	0.47	31.18	0.41	50.93	0.21
mPLUG-Owl	53.50	0.02	68.53	0.07	31.13	0.09	65.75	0.03	36.87	0.12	42.78	0.34	49.76	0.11
PandaGPT	49.13	0.47	26.27	0.15	26.40	0.21	47.25	0.13	33.80	0.52	38.88	0.40	36.96	0.31
IB-LLM	52.13	0.00	61.87	0.07	29.53	0.11	55.00	0.03	33.60	0.03	41.42	0.04	45.59	0.05
LA-V2	64.50	0.26	60.20	0.07	29.80	0.11	64.00	0.03	39.27	0.42	41.36	0.02	49.86	0.15
mmGPT	52.17	0.00	51.93	0.08	28.53	0.09	58.25	0.10	32.33	0.00	41.54	0.00	44.13	0.05
Shikra	90.63	0.14	**78.13**	0.08	31.87	0.08	64.25	0.03	49.40	0.10	41.36	0.00	**59.27**	0.07
Lynx	96.23	0.04	72.73	0.06	**33.00**	0.09	63.75	0.05	43.00	0.15	35.98	0.17	57.44	0.09
Cheetor$_V$	79.07	0.26	58.07	0.17	29.93	0.21	62.00	0.05	40.67	0.54	34.08	0.10	50.64	0.22
Cheetor$_{L_2}$	56.13	0.08	63.33	0.10	29.80	0.16	58.50	0.06	34.40	0.05	41.12	0.17	47.21	0.10
BLIVA	83.30	0.27	59.33	0.14	31.40	0.12	63.75	0.10	42.40	0.19	42.25	0.25	53.74	0.18

Table 18: Evaluation results on cross-modal inference.

Model	**Image Captioning**				**Avg.**
	COCO	**TextCaps**	**NoCaps**	**Flickr30K**	
BLIP-2$_F$	**97.48**	**41.56**	**83.57**	**74.63**	**74.31**
InstructBLIP$_F$	54.79	16.38	45.31	58.63	43.78
InstructBLIP$_V$	30.97	17.16	30.18	30.77	27.27
LLaVA$_V$	47.16	21.79	42.43	35.78	36.79
LLaVA$_{L_2}$	50.74	24.49	45.44	37.45	39.53
MiniGPT4	57.20	29.19	58.71	44.71	47.45
mPLUG-Owl	59.36	24.25	48.43	46.61	44.66
PandaGPT	2.24	0.95	1.12	1.93	1.56
IB-LLM	38.15	16.45	32.83	23.14	27.64
LA-V2	44.60	22.10	41.06	36.08	35.96
mmGPT	35.50	18.68	33.20	23.45	27.71
Shikra	41.01	19.76	37.42	28.91	31.78
Lynx	80.04	34.43	77.31	51.04	60.71
Cheetor$_V$	86.90	32.70	73.99	52.88	61.62
Cheetor$_{L_2}$	72.80	21.64	44.39	36.63	43.86
BLIVA	62.23	36.72	64.21	46.90	52.51

Table 19: Evaluation results on visual description.

For models with 100M-1B trainable parameters, Q-Former or Perceiver are trained and applied as connection modules, which enhance the capacity of models across various tasks.

In the context of LLM trainable parameters, fine-tuning all the parameters of LLMs or adding an additional small amount of trainable parameters to the LLMs does not contribute to the overall performance of LVLMs. However, adding a sufficient and appropriate number of trainable parameters to the LLM may have the potential to improve models' performances on visual language tasks.

With regard to the number of visual tokens shown in Figure 9, the model's performance shows a decline with a visual token count of 1 and 10, performs optimally at 32 but deteriorates when further increased to 64 or 256, which still outperforms models with only 1 or 10 visual tokens. This indicates that a marginal increase in the number of visual tokens may be beneficial for enhancing model performance. However, the observed outcomes that poor performance exhibited by models with 1-10 VT are attributed to the joint influence of two factors: the use of ImageBind visual encoder and the restricted number of visual tokens. Since there are only three models in this range and two of them utilize the ImageBind encoder, distinguishing whether the observed degradation is primarily

Model	VQA-MT			VisDial			Avg.	
	Acc	Instability	Corr	Acc	Instability	Corr	Acc	Instability
Generation Evaluation								
BLIP-2$_F$	<u>67.97</u>	0.20	-0.26	**55.53**	0.24	-0.93	**61.75**	0.22
InstructBLIP$_F$	**68.67**	0.19	-0.57	<u>52.51</u>	0.24	-0.84	<u>60.59</u>	0.22
InstructBLIP$_V$	56.58	0.48	-0.65	40.68	0.61	-0.97	48.63	0.55
LLaVA$_V$	40.06	0.76	0.16	31.15	0.77	-0.92	35.61	0.77
LLaVA$_{L_2}$	50.47	0.54	-0.68	42.11	0.46	-0.82	46.29	0.50
MiniGPT4	43.98	0.23	-0.31	35.05	0.66	-0.89	39.52	0.45
mPLUG-Owl	38.66	0.77	0.71	31.85	0.80	-0.83	35.23	0.79
PandaGPT	34.73	0.64	0.22	33.44	0.63	-0.68	34.09	0.64
IB-LLM	37.24	0.66	0.14	33.26	0.69	-0.78	35.25	0.68
LA-V2	38.88	0.72	-0.04	32.00	0.76	-0.85	35.44	0.74
mmGPT	34.92	0.80	0.86	28.75	0.90	-0.57	31.84	0.85
Shikra	43.33	0.67	0.68	27.12	0.91	-0.93	35.23	0.79
Lynx	54.59	0.38	-0.71	39.43	0.60	-0.84	47.01	0.49
Cheetor$_V$	44.40	0.55	-0.57	36.14	0.59	-0.89	40.27	0.57
Cheetor$_{L_2}$	41.36	0.49	-0.72	39.80	0.39	-0.74	40.58	0.44
BLIVA	48.83	0.57	-0.08	30.80	0.75	-0.95	39.82	0.66
Likelihood Evaluation								
BLIP-2$_F$	71.52	0.04	-0.10	53.62	0.04	-0.06	62.57	0.04
InstructBLIP$_F$	77.06	0.06	0.23	57.34	0.04	-0.67	67.20	0.05
InstructBLIP$_V$	**78.06**	0.04	-0.21	**59.30**	0.04	-0.66	**68.68**	0.04
LLaVA$_V$	61.32	0.05	0.47	43.24	0.04	-0.83	52.28	0.05
LLaVA$_{L_2}$	56.24	0.06	0.65	40.97	0.03	-0.46	48.61	0.05
MiniGPT4	63.97	0.06	0.67	44.14	0.05	-0.54	54.06	0.06
mPLUG-Owl	52.38	0.04	0.68	38.57	0.03	-0.69	45.48	0.04
PandaGPT	43.71	0.18	0.91	39.21	0.09	0.42	41.46	0.14
IB-LLM	43.11	0.03	0.50	35.86	0.02	-0.61	39.49	0.03
LA-V2	47.29	0.08	0.55	39.49	0.04	-0.30	43.39	0.06
mmGPT	47.52	0.06	-0.55	38.57	0.03	-0.69	43.05	0.05
Shikra	69.15	0.06	0.29	49.76	0.03	-0.65	59.46	0.05
Lynx	67.75	0.08	0.29	52.22	0.05	-0.70	59.99	0.07
Cheetor$_V$	66.01	0.06	0.53	49.22	0.06	0.29	57.62	0.06
Cheetor$_{L_2}$	51.86	0.10	-0.69	41.82	0.05	-0.78	46.84	0.08
BLIVA	<u>77.92</u>	0.05	0.18	<u>58.24</u>	0.04	-0.65	<u>68.08</u>	0.05

Table 20: Evaluation results on multi-turn Dialogue. "Corr" represents the correlation coefficient between the model performance and the number of dialogue turns.

Backbone	**FlanT5-xl**		**LLaMA-7B**			**Vicuna-7B**		
Model	BLIP-2	InstructBLIP	ImageBind-LLM	LA-V2	mPLUG-Owl	Cheetor	BLIVA	InstructBLIP
Hit Rate	100.0	99.99	99.94	85.14	62.86	99.97	99.77	99.99
Hit Rate+	100.0	100.0	100.0	100	100	100.0	100.0	100.0

Backbone	**Vicuna-7B**	**Vicuna-7B+**		**Vicuna-7B+Δ**		**LLaMA2-7B-Chat**		**OpenFlamingo**
Model	MiniGPT-4	LLaVA	Shikra	Lynx	PandaGPT	LLaVA	Cheetor	mmGPT
Hit Rate	100.0	85.32	65.42	94.41	99.41	100.0	99.31	95.71
Hit Rate+	100.0	100.0	97.72	100.0	99.97	100.0	100.0	99.97

Table 21: Complete results for Table 3. "+Δ" represents delta tuning with parameter-efficient modules like LoRA and adapters.

attributable to the suboptimal performance of the ImageBind encoder or limited visual tokens remains uncertain. Moreover, increasing the number of visual tokens from 32 does not inherently lead to augmented model capability.

C.4 Effect of Dataset

High-Quality Pre-training Dataset To quantitatively assess the impact of the COCO dataset during the pre-training stage, we conduct an evaluation using two groups of models, one group includes three models (BLIP2, mPlug-Owl, and Lynx), while the other group consists of two models (LLaVA and MiniGPT4) not trained with COCO. For fair evaluation, we choose 6 in-domain tasks (containing images from COCO) and 6 out-domain tasks (not containing images from COCO) across perception and cognition capacity. To mitigate the influence of score fluctuations across tasks, we

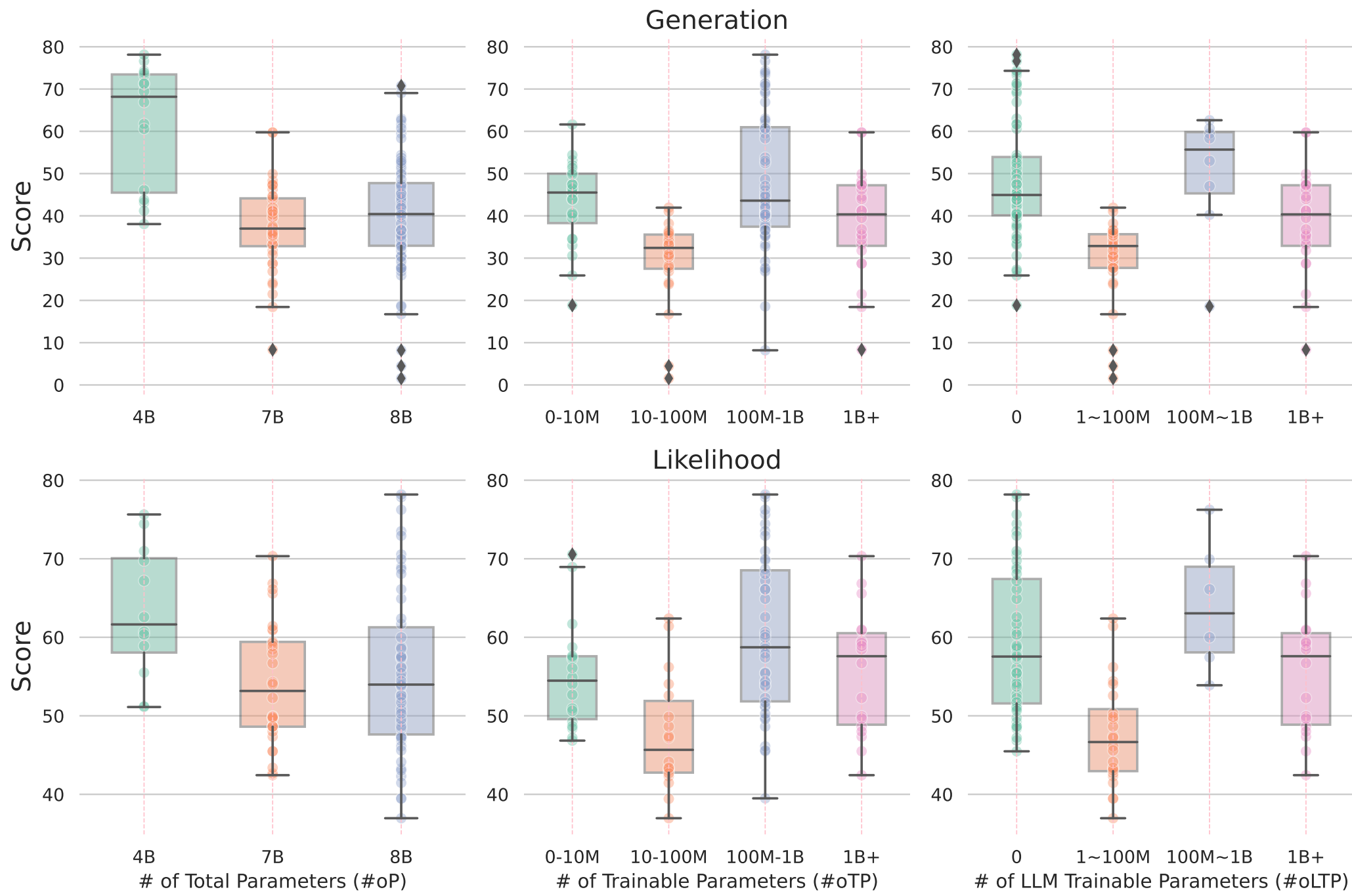

Figure 8: Performance under different numbers of total parameters (#oP), trainable parameters (#oTP), and LLM trainable parameters (#oLTP). Note that, regarding the "# of Total Parameters (#oP)", models around 4B parameters include only BLIP2-FlanT5-XL and InstructBLIP-FlanT5-XL.

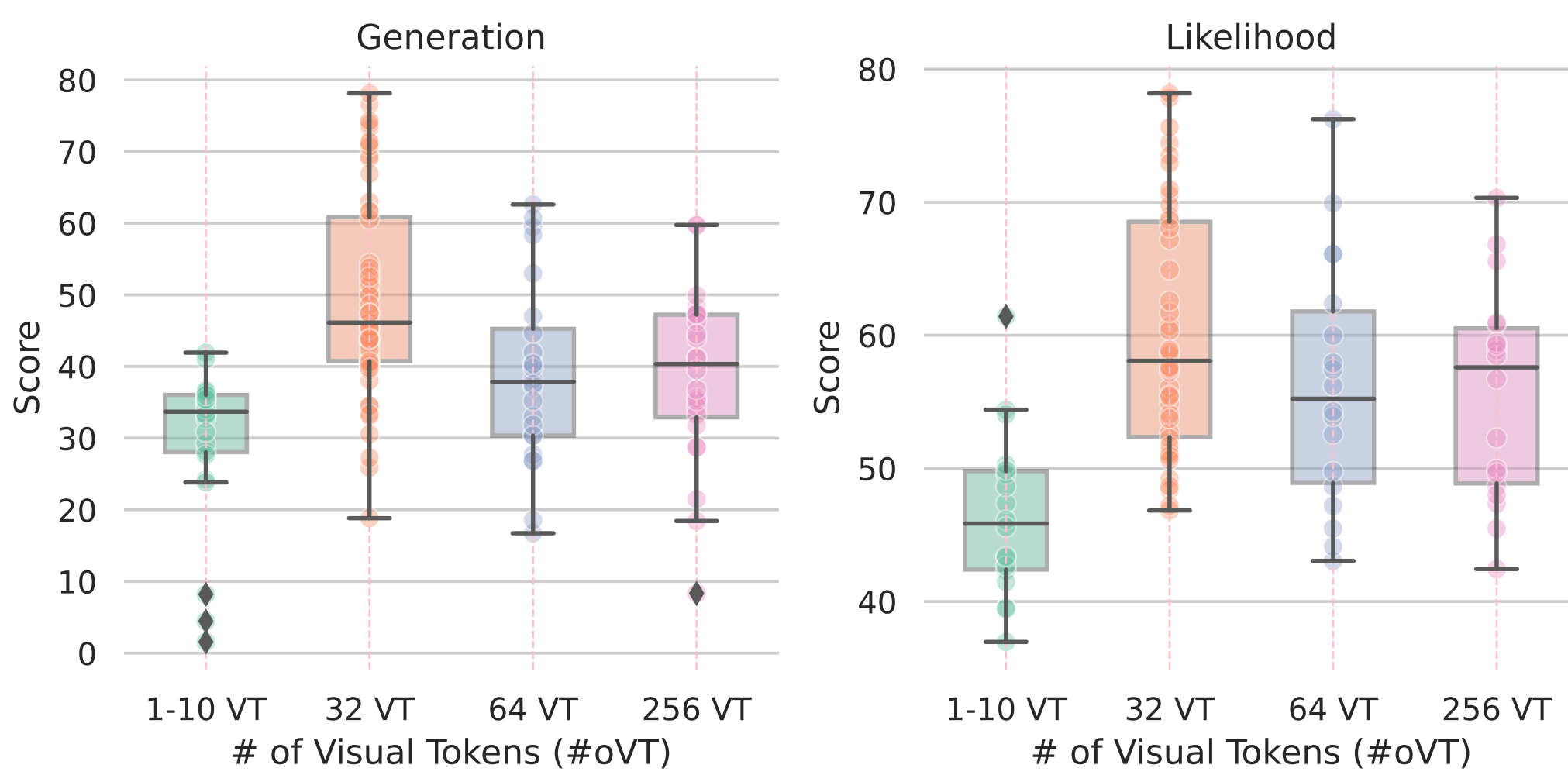

Figure 9: Performance under different numbers of visual tokens (#oVT). It is noteworthy that the group of 1-10VT consists of only two models with 1 visual token (1VT) and one model with 10 visual tokens (10VT). Specifically, 1VT models encompass PandaGPT and IB-LLM, where both of them apply an ImageBind visual encoder.

utilize the average rank within each group as a metric to evaluate their collective performance on particular tasks. The selected tasks and the average rank for each group are listed in Table 22.

Scaling Up Pre-Training Dataset To explore the influence of high-quality pre-training data, we select two groups of models: one group (including LLaVA$_V$, MiniGPT4, ImageBind-LLM, and

Model Group	In-Domain Task					
	$MSCOCO_{mci}$	**$MSCOCO_{goi}$**	**COCO-Caption**	**Flickr30K**	**$MSCOCO_{itm}$**	**$MSCOCO_{its}$**
Pre-Training w. COCO	**6**	5.67	**8**	**7.33**	**6.33**	**5**
Pre-Training w.o. COCO	6.5	**5.5**	8.5	9	12	7
Model Group	**Out-Domain Task**					
	Pets37	**Flowers102**	**TextCaps**	**NoCaps**	**Wikihow**	**Winoground**
Pre-Training w. COCO	**3.67**	**3.33**	7.67	7.67	**6.67**	**3.33**
Pre-Training w.o. COCO	8	7	**7**	**7.5**	8.5	4.5

Table 22: Average rank of model groups in in-domain and out-domain tasks.

Model	Generation			Likelihood
	Instruct	Option Order	Option Mark	Instruct
$BLIP2_F$	0.029	0.276	0.107	0.037
$InstructBLIP_F$	0.028	0.242	0.105	0.028
$InstructBLIP_V$	0.038	0.414	0.182	0.018
$LLaVA_V$	0.197	0.606	0.299	0.105
$LLaVA_{L_2}$	0.141	0.464	0.178	0.090
MiniGPT4	0.113	0.647	0.194	0.043
mPLUG-Owl	0.330	0.706	0.406	0.046
PandaGPT	0.125	0.592	0.198	0.117
IB-LLM	0.159	0.702	0.498	0.024
LA-V2	0.382	0.682	0.518	0.032
mmGPT	0.578	0.763	0.601	0.030
Shikra	0.028	0.617	0.206	0.054
Lynx	0.069	0.375	0.195	0.052
$Cheetor_V$	0.177	0.666	0.356	0.076
$Cheetor_{L_2}$	0.051	0.476	0.163	0.058
BLIVA	0.128	0.610	0.204	0.023
Average	**0.161**	**0.552**	**0.276**	**0.049**

Table 23: Instability of models caused by different random perturbations.

mPLUG-Owl) utilizes data filtered based on rules or CLIP like CC (Sharma et al., 2018) and LAION (Schuhmann et al., 2021), while the other group (including LA-V2, Shikra, BLIP2, and Lynx) is pre-trained using relatively high-quality data like COCO (Chen et al., 2015) and BlipCap-Filt (Li et al., 2022) as indicated in Table 8.

Instruct-Tuning Dataset Based on the data in Table 8, we calculate the number of instruction-tuning datasets for each model and plot the relationship between the number of instruction-tuning datasets and the average rank.

C.5 Instability

Table 23 provides the complete results of models' instability caused by different perturbations. Under the generation evaluation, all models are most sensitive to the order of options, followed by the option marks, and lastly, random instructions. FlanT5 models are the most stable models under the generation evaluation, showing that FlanT5 can well comprehend the multiple-choice questions. For likelihood evaluation, all models are stable since the evaluation strategy directly utilizes the characteristics of generative models.

To further perceive the influence of instruction perturbation on the answer accuracy, we analyze the above instruction perturbation results. As we employ different instructions to describe the same task, the accuracy of samples that follow each instruction can be calculated. For the accuracy of each instruction, we adopt the difference between the maximum and minimum accuracies to represent the model's instability level towards the instruction. The results are shown in Table 24. We discover that all models exhibit some fluctuations in accuracy, illustrating that LVLMs are sensitive to de-

Model	Generation	Likelihood
BLIP2$_F$	6.47	6.96
InstructBLIP$_F$	3.48	5.97
InstructBLIP$_V$	4.48	5.97
LLaVA$_V$	3.48	6.47
LLaVA$_{L_2}$	1.99	7.46
MiniGPT4	3.48	5.97
mPLUG-Owl	4.98	6.47
PandaGPT	5.47	6.47
IB-LLM	7.46	3.98
LA-V2	3.48	3.98
mmGPT	10.45	4.48
Shikra	12.94	2.99
Lynx	6.97	9.95
Cheetor$_V$	3.48	5.97
Cheetor$_{L_2}$	6.47	7.46
BLIVA	1.99	9.95
Average	**5.44**	**6.28**

Table 24: The difference between the maximum and minimum accuracies of all instruction groups.

signed prompts. However, the fluctuations in accuracy under generation and likelihood evaluation of most LVLMs are both within an acceptable range. There are still models exhibiting fluctuations in accuracy exceeding 10%, indicating the restricted instruction-following capabilities of LVLMs. In general, LVLMs require further improvements to enhance its ability to understand and follow diverse instructions.

C.6 Option Preference

Option preference is a phenomenon in our benchmark that when uncertain about the answer, LVLMs prefer a particular option regardless of options' content. We verify the option preference inside the LVLMs in Figure 10. It has been observed that ImageBind-LLM, Shikra, and BLIVA exhibit a preference for option "A" when confronted with uncertainty. MiniGPT4, mPLUG-Owl, PandaGPT, LA-V2 and mmGPT show a strong preference for option "B". Other LVLMs show no obvious preference in this task. It's worth noting that predicted choice distribution under the likelihood evaluation method has no preference, as all options are considered in an unordered state.

The phenomenon of option preference contributes to the instability from random option order but reduces that from random instruction and option mark (as mentioned in Section 4.3.5). Concretely, when LVLMs are uncertain about answers, they select the ceratin option repeatedly for the essentially identical questions. As the option contents have been shuffled in random option mark mode, the LVLMs are regarded as selecting distinct answers. Regarding random instruction and option mark situations, LVLMs are firm in their answers regardless variation of question form.

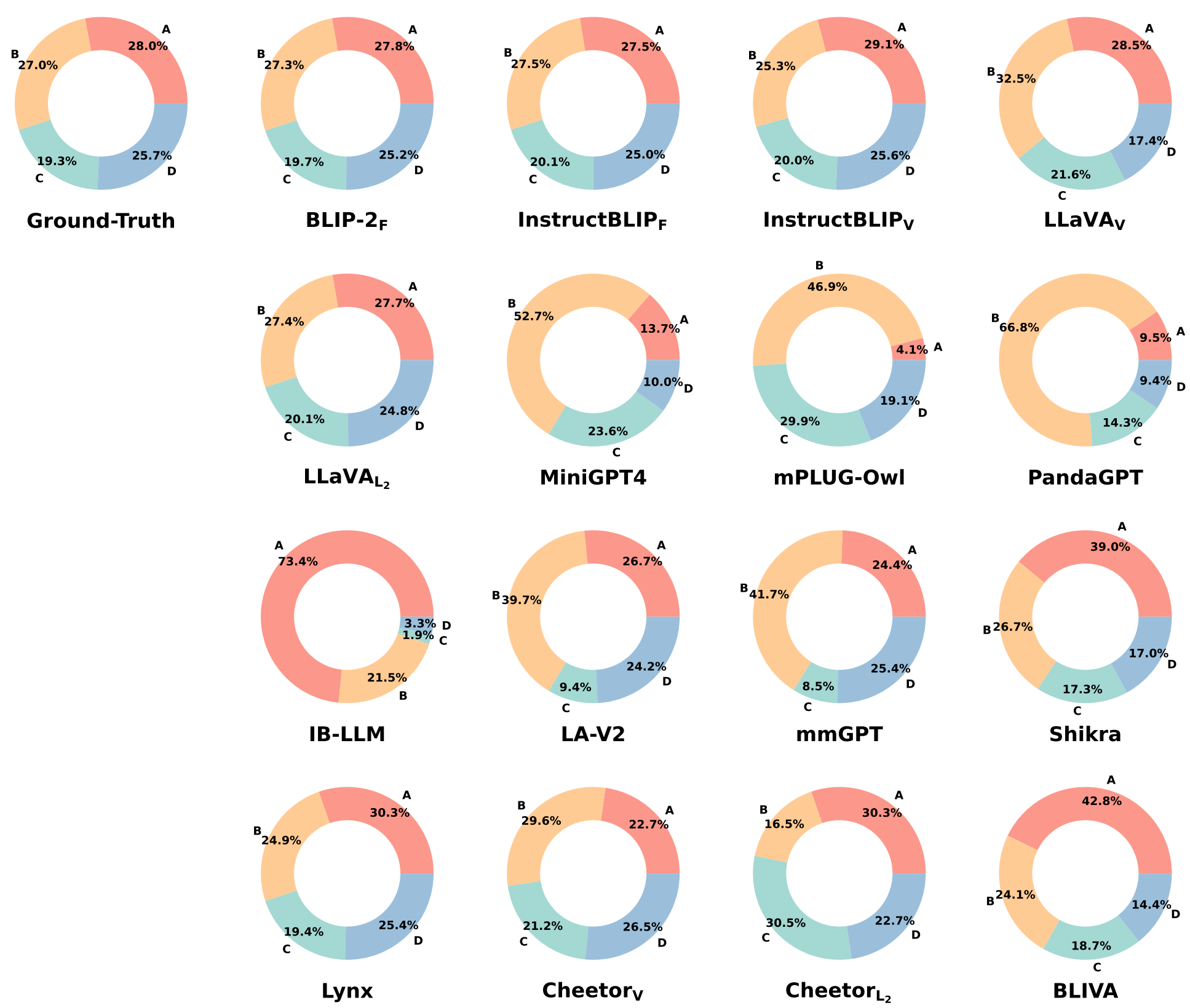

Figure 10: The choice distribution of ground-truth answers and prediction of all LVLMs in COCO image text selection task under generation method.

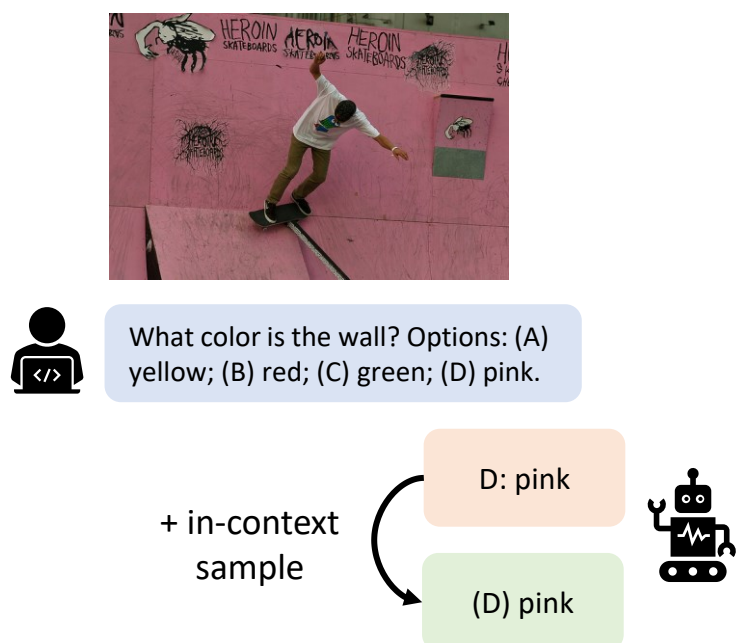

(a) mPLUG-Owl

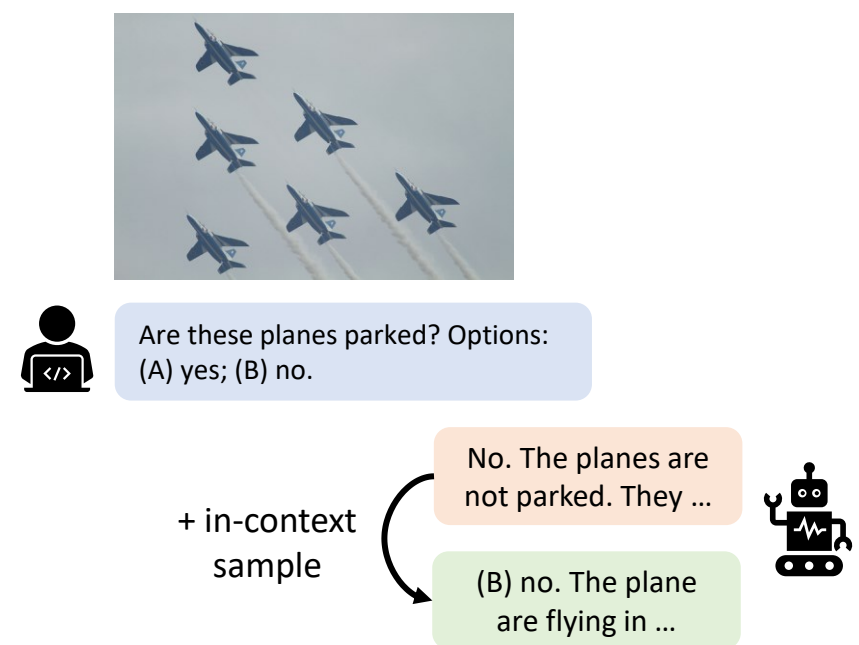

(b) LA-V2

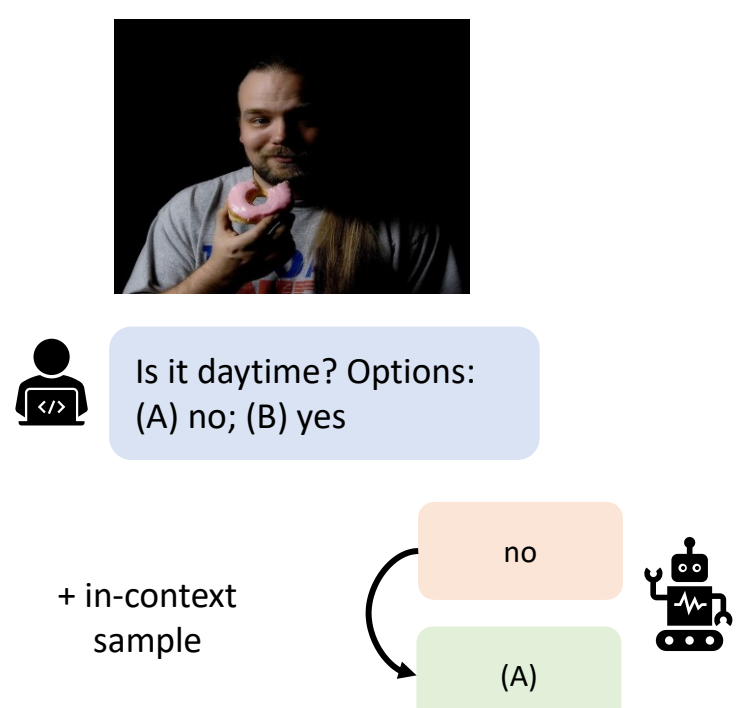

(c) Shikra

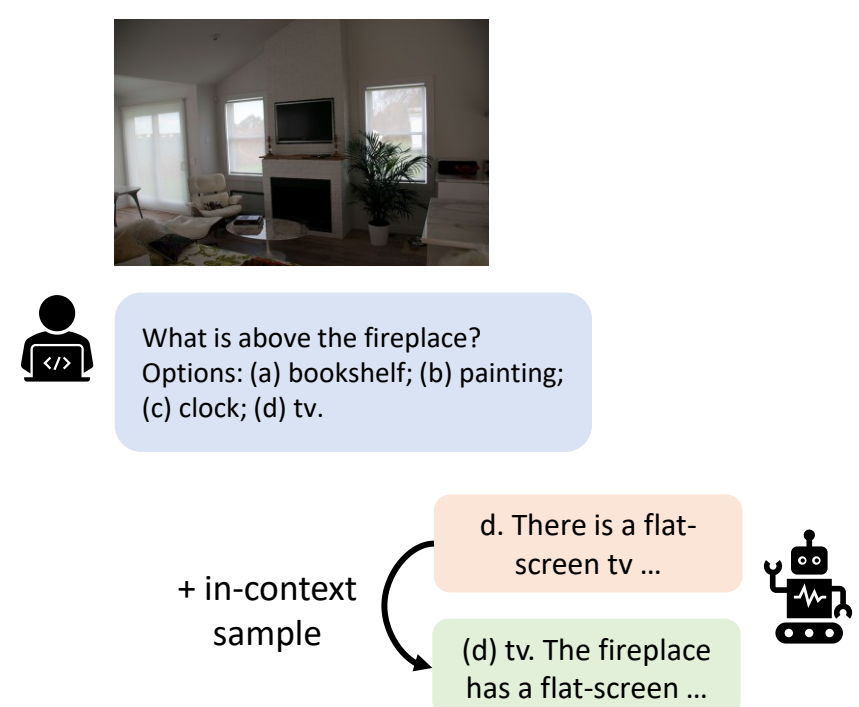

(d) Lynx

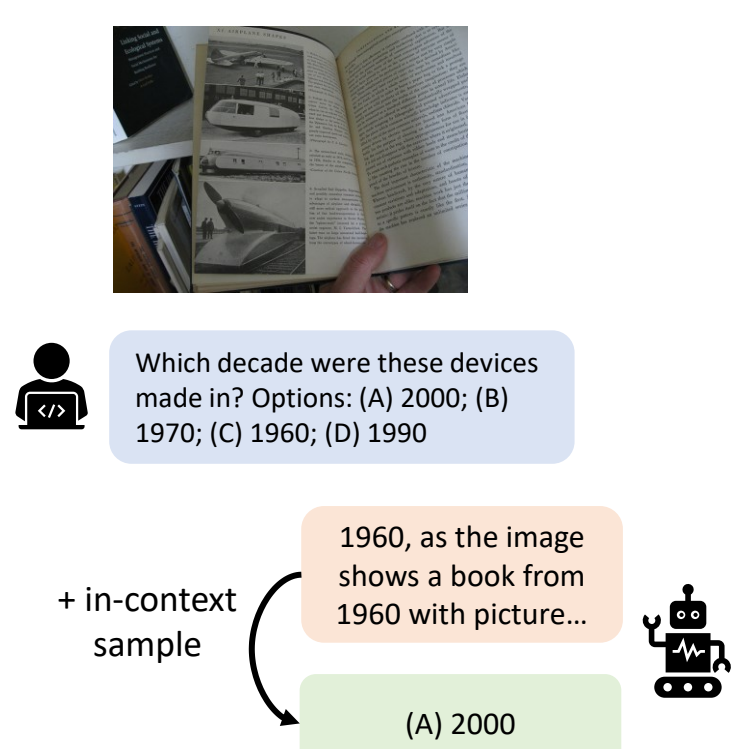

(e) LLaVA

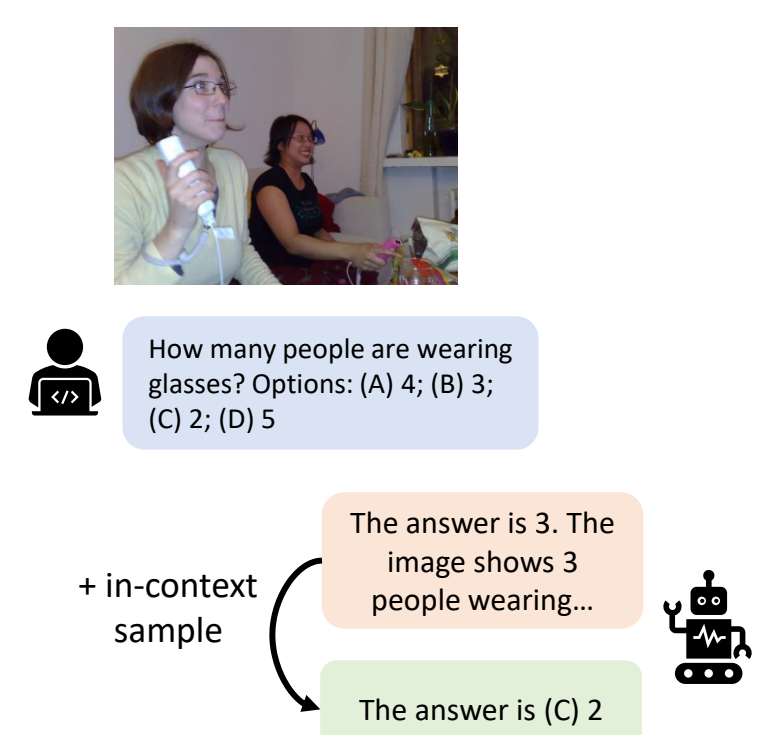

(f) mmGPT

Figure 11: Case study of the effect of in-context samples, the instruction used is "Take a close look at the image and question, and then choose the correct option" which is omitted for simplicity.